Chapter 2

Constricted Variational Density Functional Theory Approach to the Description of Excited States

Florian Senn, Issaka Seidu and Young Choon Park

Additional information is available at the end of the chapter

http://dx.doi.org/10.5772/intechopen.70932

Abstract

The aim of this chapter is to present constricted variational density functional theory (CV-DFT), a DFT-based method for calculating excited-state energies. This method involves constructing from the ground-state orbitals, a new set of 'occupied' excited-state orbitals. Consequently, a constraint is applied to ensure that exactly one electron is fully transferred from the occupied to the virtual space. This constraint also prevents a collapse to a lower state. With this set of orbitals, one obtains an electron density for the excited-state and therewith the CV-DFT excitation energy. This excitation energy can now be variationally optimized. With our successful applications to systems differing in the type of excitation, namely, charge-transfer, charge-transfer in disguise, and Rydberg excitations, as well as in size, we demonstrate the strengths of the CV-DFT method. Therewith, CV-DFT provides a valid alternative to calculate excited-state properties, especially in cases where TD-DFT has difficulties. Finally, our studies have shown that the difficulties arising in the TD-DFT excited states are not necessarily stemming from the functional used, but from the application of these standard functionals in combination with the linear response theory.

Keywords: CV-DFT, excited state, charge-transfer, Rydberg excitations, ZnBC-BC

1. Introduction

The behavior of atoms and polyatomic systems in the excited-state are of immense importance in the studies of several photophysical phenomena. Thus, the search for methods to study systems in their electronically excited state is the subject of ongoing research [1–13]. Resultantly, there are several methods to choose from within certain consideration such as system size, expected level of accuracy and nature of initial and final electronic state of the system under study. Therefore, some background knowledge is necessary for the accurate treatment of excited states with the available methods. These methods fall under different families, and

the *ab initio* wave function family of methods includes multi-reference configuration interaction (MRCI) [14], multi-configurational self-consistent field (MCSCF) [15, 16], complete active space self-consistent field (CASSCF) [17], time-dependent Hartree-Fock (TD-HF) [18–21], restricted active space self-consistent field (RASSCF) [22], RASPT2 [23], complete active space second-order perturbation theory (CASPT2) [24], equation-of-motion coupled cluster (EOMCC) [25], *n*-electron valence state perturbation theory (NEVPT) [26], spectroscopically oriented configuration interaction (SORCI) [27] and coupled cluster (CC) theory [28, 29].

However, the focus of this book is the Kohn-Sham density functional theory (DFT) [30] and methods based on it. In this chapter, our attention is on the calculation of excited states. Excited-state studies within DFT gained considerable attention owing to the increasing success of DFT in ground-state studies. Significant research effort toward the development of excited-state methods has resulted in a variety of approaches varying in both major and minor details, each method having its own advantages and disadvantages. The result of this endeavor includes self-consistent-field DFT (ΔSCF-DFT) [31–33] with extensions [34–36], time-dependent DFT [40–44], ensemble DFT [37–39, 45–47], constrained orthogonality method (COM) [48–50], restricted open-shell Kohn-Sham (ROKS) [47, 51, 52], constrained DFT (CDFT) [53], 'taking orthogonality constraints into account' (TOCIA) [54, 55], maximum overlap method (MOM) [56, 57], constricted variational density functional theory (CV-DFT) [58] and extensions [59–62], orthogonality constrained DFT (OCDFT) [63] and guided SCF [64] among others. However, the most widely used by both expert and nonexpert is TD-DFT in the form of linear response adiabatic time-dependent DFT [40, 41, 65–69] (which we will refer to as TD-DFT) due to its successes.

The strengths and weaknesses of TD-DFT are well known and understood through extensive benchmark studies carried out over the years. The strengths explain its wide usage by delivering 'an excellent compromise between computational efficiency and accuracy' [70]. The weaknesses explain the ongoing fundamental studies searching for solutions in the cases where TD-DFT is found lacking. These include its deficiency in describing Rydberg transitions [71–74], charge-transfer (CT) transitions [75–84] and electronic transition with significant double contribution [42, 43, 83–87]. TD-DFT is a formally exact theory; however, its practical application relies on the adiabatic formalism where use is made of the available ground-state exchange-correlation (*XC*) functionals [71, 82, 88–90]. As a result, one can necessarily trace all the problems encountered in the application of TD-DFT to this approximation. The numerous research attempts to remedy the pitfalls in TD-DFT are classified as follows:

1. Finding the *XC* functionals with the correct short- and long-range behavior or going beyond the adiabatic approximation.
2. Developing new DFT-based excited-state methods.

An often-encountered problem with the development of specialized functionals is that it usually performs very well for the purpose for which it was originally developed but unimaginably erratic for any other situation [71–74, 77, 79, 82, 88, 91–98].

Our contribution to this area of research is in the development of the constricted variational DFT (CV-DFT) [58–62], which combines the strengths of ΔSCF-DFT and TD-DFT methods without the need for 'specialized' functionals.

In this chapter, we will explain the idea and theory of CV-DFT, before we have a look at different examples, where CV-DFT has been applied for transitions of Rydberg and charge-transfer type following the publications [99–103].

2. Theory

In this chapter, we review the theoretical framework of CV-DFT in a nutshell. We refer to the original publications [58–62, 104] for a more in-depth description.

2.1. The CV-DFT scheme

Here, we only consider the excitation from the closed-shell ground state described with single Slater determinant, $\Psi^0 = \left|\phi_1\phi_2\ldots\phi_i\ldots\phi_{n_{\text{occ}}}\right|$, where n_{occ} is the number of occupied orbitals. CV-DFT starts from the ansatz which describes the excitation as an admixture of occupied $\{\phi_i; i = 1, \cdots, n_{\text{occ}}\}$ and virtual $\{\phi_a; a = 1, \cdots, n_{\text{vir}}\}$ ground-state orbitals [105]:

$$\phi_i' = \sum_a^{n_{\text{vir}}} U_{ai}\phi_a \tag{1}$$

where ϕ_i' is the excited-state orbital and n_{vir} the number of virtual orbitals. The transition matrix, $\mathbf{U}$, only mixes between occupied and virtual orbitals ($U_{ij} = U_{ab} = 0$) and is skew symmetric ($U_{ai} = -U_{ia}$). In CV-DFT, we use the exponential expansion of $\mathbf{U}$ which leads to the unitary transformation $\mathbf{Y}$:

$$\mathbf{Y} = \exp(\mathbf{U}) = \sum_{k=0}^{\infty} \frac{\mathbf{U}^k}{k!}. \tag{2}$$

Thus, once the transition matrix, $\mathbf{U}$, is determined, a new set of orbitals is obtained over the unitary transformation

$$\begin{pmatrix} \phi_{\text{occ}}' \\ \phi_{\text{vir}}' \end{pmatrix} = \left(\sum_{k=0}^{\infty} \frac{\mathbf{U}^k}{k!}\right) \begin{pmatrix} \phi_{\text{occ}} \\ \phi_{\text{vir}} \end{pmatrix}. \tag{3}$$

Due to the properties of the transition matrix, $\mathbf{U}$, the 'occupied' excited-state orbitals can be written as

$$\phi_i^{'} = \sum_j^{n_{\text{occ}}} Y_{ji}\phi_j + \sum_a^{n_{\text{vir}}} Y_{ai}\phi_a. \tag{4}$$

The corresponding excited-state density becomes

$$\rho'(1,1') = \sum_{i}^{n_{\text{occ}}} \phi_i'(1)\phi_i'(1')$$

$$= \sum_{i}^{n_{\text{occ}}} \phi_i(1)\phi_i(1') + \sum_{a}^{n_{\text{vir}}}\sum_{i}^{n_{\text{occ}}} \Delta P_{ai}\left[\phi_i(1)\phi_a(1') + \phi_a(1)\phi_i(1')\right] \tag{5}$$

$$+ \sum_{i}^{n_{\text{occ}}}\sum_{j}^{n_{\text{occ}}} \Delta P_{ij}\phi_i(1)\phi_j(1') + \sum_{a}^{n_{\text{vir}}}\sum_{b}^{n_{\text{vir}}} \Delta P_{ab}\phi_a(1)\phi_b(1')$$

with the change in density matrix (ΔP). Later, one is given by

$$\Delta P_{aj} = \sum_{i}^{n_{\text{occ}}} Y_{ai}Y_{ji} \tag{6}$$

$$\Delta P_{jk} = \sum_{i}^{n_{\text{occ}}} \left(Y_{ji}Y_{ki} - \delta_{jk}\right) \tag{7}$$

$$\Delta P_{ab} = \sum_{i}^{n_{\text{occ}}} Y_{ai}Y_{bi}. \tag{8}$$

In CV-DFT, we apply the important condition that one electron is fully transferred from occupied into virtual spaces. This condition can be written as the following equation:

$$\sum_{a}^{n_{\text{vir}}} \Delta P_{aa} = 1 \quad \text{and} \quad \sum_{i}^{n_{\text{occ}}} \Delta P_{ii} = -1. \tag{9}$$

It should be noted that in CV-DFT we describe the excited state with a single Slater determinant. Thus, we obtain the mixed and triplet states. While this is uncritical for triplet excitations, for the singlet transition energy, we have to account for this by using the relation (which is also referred to as sum rule) [61]

$$\Delta E_S = 2\Delta E_M - \Delta E_T. \tag{10}$$

2.2. CV(*n*)-DFT

The *n*th-order CV-DFT, CV(*n*)-DFT, is determined from the maximum order of **U** in the CV-DFT energy description. To understand how the order of the applied transition matrix, **U**, affects the excited-state energies, it is beneficial to discuss two extreme cases—second ($n = 2$)-order and infinite ($n = \infty$)-order CV-DFT.

The second-order CV-DFT (CV(2)-DFT) limits the **U** up to the second order in the Kohn-Sham energy description. For simplicity, the occupied excited-state orbitals in Eq. (4) are approximated to the second order in **U**:

http://dx.doi.org/10.5772/intechopen.70932

$$\phi_i^{'} = \phi_i + \sum_a^{n_{\text{vir}}} U_{ai}\phi_a - \frac{1}{2}\sum_j^{n_{\text{occ}}}\sum_a^{n_{\text{vir}}} U_{ai}U_{aj}\phi_j + O\left[U^{(3)}\right] \quad . \tag{11}$$

With these orbitals, some higher order contributions in **U** can arise in the density and therewith also in the energy, but we only keep up to the second order in **U**, as the contribution of higher order terms is negligible [60]. The second-order CV-DFT energy expression becomes

$$\begin{aligned} E_{KS}[\boldsymbol{\rho}'(1,1')] \quad &= E_{KS}\left[\rho^0\right] + \sum_{ai} U_{ai}U_{ai}^*\left(\varepsilon_a^0 - \varepsilon_i^0\right) + \sum_{ai} U_{ai}U_{bj}^* K_{ai,bj} \\ &+ \frac{1}{2}\sum_{ai}\sum_{bj} U_{ai}U_{bj}K_{ai,jb} + \frac{1}{2}\sum_{ai}\sum_{bj} U_{ai}^*U_{bj}^*K_{ai,jb} + O\left[U^{(3)}\right] \end{aligned} \tag{12}$$

where the two-electron integral is composed of a Coulomb and an exchange-correlation part:

$$K_{pq,st} = K_{pq,st}^{C} + K_{pq,st}^{XC} \tag{13}$$

with

$$K_{pq,st}^{C} = \int\int \psi_p(1)\psi_q(1)\frac{1}{r_{12}}\psi_s(2)\psi_t(2)dv_1dv_2. \tag{14}$$

The exchange-correlation integral is further decomposed into the local (KS) and nonlocal (HF):

$$K_{pq,st}^{XC(KS)} = \int \psi_p(r_1)\psi_q(r_1)f(r_1)\psi_s(r_1)\psi_t(r_1)dr_1 \tag{15}$$

and

$$K_{pq,st}^{XC(HF)} = -\int\int \psi_p(1)\psi_q(1)\frac{1}{r_{12}}\psi_s(2)\psi_t(2)dv_1dv_2 \tag{16}$$

where $f(r_1)$ represents the regular energy kernel. We have shown that CV(2)-DFT is equivalent to TD-DFT [59, 106] within the Tamm-Dancoff approximation (TDA) [107].

In the infinite-order theory (CV(∞)-DFT), the new set of excited-state orbitals is obtained taking the sum in Eq. (3) to infinite order. These excited-state orbitals can be written in the convenient form of natural transition orbitals (NTO) [108]. For this, we decompose the transition matrix, **U**, into its singular values. Here, we also used a spin-adapted form for further description of the different spin states in the excited-state calculation:

$$\mathbf{U}^{\sigma\alpha} = \mathbf{V}^{\sigma\sigma}\Sigma(\mathbf{W}^{\alpha\alpha})^{\mathrm{T}} \tag{17}$$

where $\Sigma_{ii} = \gamma_i$ and $\sigma \in \{\alpha, \beta\}$ depend on spin state (mixed and triplet states, respectively). This leads to the occupied and virtual NTOs as

$$\phi_i^{o_\alpha} = \sum_j^{n_{\text{occ}}} (\mathbf{W}^{\alpha\alpha})_{ji} \phi_j^{\alpha} \tag{18}$$

$$\phi_i^{v_\sigma} = \sum_a^{n_{\text{vir}}} (\mathbf{V}^{\sigma\sigma})_{ai} \phi_a^{\sigma}. \tag{19}$$

The resulting matrix **W** rotates ground-state KS orbitals as j runs over the occupied ground-state orbitals to give the corresponding ith 'occupied' NTO orbital ($\phi_i^{o_\alpha}$). For its virtual counterpart ($\phi_i^{v_\sigma}$), **V** does the similar role as **W** with a running over the virtual ground-state orbitals. With these NTOs, we can rewrite Eq. (4) for the 'occupied' excited-state orbitals as

$$\phi_i^{'} = \cos[\gamma_i]\phi_i^{o_\alpha} + \sin[\gamma_i]\phi_i^{v_\sigma}. \tag{20}$$

Also, the condition of exciting exactly one electron (Eq. (9)) is now written as

$$\sum_i^{n_{\text{occ}}} \sin(\eta\gamma_i)^2 = 1. \tag{21}$$

With the sum rule in Eq. (10), the excited-state CV(∞)-DFT energy of the mixed state becomes

$$\begin{aligned}
\Delta E_M = & \sum_i^{n_{\text{occ}}} \sin^2[\eta\gamma_i](\varepsilon_i^{v_\alpha} - \varepsilon_i^{o_\alpha}) \\
& + \frac{1}{2}\sum_i^{n_{\text{occ}}}\sum_j^{n_{\text{occ}}} \sin^2[\eta\gamma_i]\sin^2\left[\eta\gamma_j\right]\left(K_{i^{o_\alpha}i^{o_\alpha}j^{o_\alpha}j^{o_\alpha}}K_{i^{v_\alpha}i^{v_\alpha}j^{v_\alpha}j^{v_\alpha}} - 2K_{i^{o_\alpha}i^{o_\alpha}j^{v_\alpha}j^{v_\alpha}}\right) \\
& + \frac{1}{2}\sum_i^{n_{\text{occ}}}\sum_j^{n_{\text{occ}}} \sin[\eta\gamma_i]\cos[\eta\gamma_i]\sin\left[\eta\gamma_j\right]\cos\left[\eta\gamma_j\right]\left(K_{i^{o_\alpha}i^{v_\alpha}j^{o_\alpha}j^{v_\alpha}} + K_{i^{o_\alpha}i^{v_\alpha}j^{v_\alpha}j^{o_\alpha}}\right) \\
& + 2\sum_i^{n_{\text{occ}}}\sum_j^{n_{\text{occ}}} \sin[\eta\gamma_i]\sin[\eta\gamma_i]\sin\left[\eta\gamma_j\right]\cos\left[\eta\gamma_j\right]\left(K_{i^{v_\alpha}i^{v_\alpha}j^{o_\alpha}j^{v_\alpha}} - K_{i^{o_\alpha}i^{o_\alpha}j^{o_\alpha}j^{v_\alpha}}\right)
\end{aligned} \tag{22}$$

whereas the triplet exited-state energy has a simpler form:

$$\begin{aligned}
\Delta E_T = & \sum_i^{n_{\text{occ}}} \sin^2[\eta\gamma_i](\varepsilon_i^{v_\beta} - \varepsilon_i^{o_\alpha}) \\
& + \frac{1}{2}\sum_i^{n_{\text{occ}}}\sum_j^{n_{\text{occ}}} \sin^2[\eta\gamma_i]\sin^2\left[\eta\gamma_j\right]\left(K_{i^{o_\alpha}i^{o_\alpha}j^{o_\alpha}j^{o_\alpha}}K_{i^{v_\beta}i^{v_\beta}j^{v_\beta}j^{v_\beta}} - 2K_{i^{o_\alpha}i^{o_\alpha}j^{v_\beta}j^{v_\beta}}\right)
\end{aligned} \tag{23}$$

The γ values out of Eq. (21) give information about the excitation character [60]. Keeping only the largest γ value in the excitation will give the most general form of single orbital

replacement [104], which is used as the ΔSCF-DFT-like scheme within the RSCF-CV(∞)-DFT formulation. This will be briefly mentioned in the next section.

2.3. SCF-CV(∞)-DFT, R-CV(∞)-DFT and RSCF-CV(∞)-DFT

In Eqs. (22, 23), we obtain the excited-state energy of the mixed and triplet state. The transition matrix, **U**, is the same as one obtains within TD-DFT (and thus the TD-DFT excitation vector is implemented in CV-DFT). In SCF-CV(∞)-DFT, **U** is optimized with the variational procedure [60]. For this step, we derived the gradient of the mixed and triplet excited state. The detailed procedures can be found in the [59–61, 104]. Further, also the orbitals which do not participate in the excitation can be changed after the excitation. We refer to this change as the relaxation of orbitals. This leads to R-CV(∞)-DFT. To account for this orbital relaxation effect, we introduced **R**, which is orthogonal to **U**, and apply it on the orbitals from Eq. (4). Therewith, the 'occupied' and 'virtual' orbitals become

$$\psi_i(1) = \phi_i(1) + \sum_{c}^{n_{\text{vir}}} R_{ci}\phi_c(1) - \frac{1}{2}\sum_{c}^{n_{\text{vir}}}\sum_{k}^{n_{\text{occ}}} R_{ci}R_{ck}\phi_k(1) \tag{24}$$

$$\psi_a(1) = \phi_a(1) - \sum_{k}^{n_{\text{occ}}} R_{ak}\phi_k(1) - \frac{1}{2}\sum_{c}^{n_{\text{vir}}}\sum_{k}^{n_{\text{occ}}} R_{ak}R_{ck}\phi_c(1). \tag{25}$$

It is possible to combine the approach of the variational optimization of the transition matrix and orbital relaxation, meaning the variational optimization of **U** and **R**, resulting in the most general form of CV-DFT (RSCF-CV(∞)-DFT). The excitation energy expression of RSCF-CV(∞)-DFT can be written for the mixed and triplet state, respectively:

$$\begin{aligned}\Delta E_M &= E_M^{\mathbf{U},\mathbf{R}}\left[\rho_0^\alpha + \frac{1}{2}\Delta\rho_M^{\mathbf{U},\mathbf{R}}, \rho_0^\beta + \frac{1}{2}\Delta\rho_M^{\mathbf{U},\mathbf{R}}\right] - E\left[\rho_0^\alpha, \rho_0^\beta\right] \\ &= \int F_{KS}\left[\rho_0^\alpha + \frac{1}{2}\Delta\rho_M^{\mathbf{U},\mathbf{R}}, \rho_0^\beta + \frac{1}{2}\Delta\rho_M^{\mathbf{U},\mathbf{R}}\right]\Delta\rho_M^{\mathbf{U},\mathbf{R}} d\nu_1\end{aligned} \tag{26}$$

$$\begin{aligned}\Delta E_T &= E_T^{\mathbf{U},\mathbf{R}}\left[\rho_0^\alpha + \frac{1}{2}\Delta\rho_T^{\mathbf{U},\mathbf{R}}, \rho_0^\beta + \frac{1}{2}\Delta\rho_T^{\mathbf{U},\mathbf{R}}\right] - E\left[\rho_0^\alpha, \rho_0^\beta\right] \\ &= \int F_{KS}\left[\rho_0^\alpha + \frac{1}{2}\Delta\rho_T^{\mathbf{U},\mathbf{R}}, \rho_0^\beta + \frac{1}{2}\Delta\rho_T^{\mathbf{U},\mathbf{R}}\right]\Delta\rho_T^{\mathbf{U},\mathbf{R}} d\nu_1\end{aligned} \tag{27}$$

where ρ_0^α and ρ_0^β are the ground-state density and $\Delta\rho^{\mathbf{U},\mathbf{R}}$ indicates the excited-state density changes including relaxation effect. The F_{KS} is the Kohn-Sham Fock operator.

Another idea is to restrict the transition matrix, **U**, in CV-DFT to the case of single NTO excitations, that is, Eq. (17) is approximated to include only one major excitation in the transition matrix. Three different forms of such restrictions on **U** were shown and discussed in the previous work [104], which referred to as SOR-R-CV(∞)-DFT, COL-RSCF-CV(∞)-DFT

	Transition U			Relaxation R		Introduced	
	Order n	Optimization	Restrictions	Order	Optimization	Singlets	Triplets
CV(2)-DFT	Second	No	No	N/A	No	T [58], I [109]	T [60], I [110]
CV(4)-DFT	Fourth	No	No	N/A	No	T [93], I [109]	T [109], I [109]
CV(∞)-DFT	∞	No	No	N/A	No	T [59], I [111]	T [60], I [60]
SCF-CV(∞)-DFT	∞	Yes	No	N/A	No	T [59], I [60]	T [60], I [104]
RSCF-CV(∞)-DFT	∞	Yes	No	Second	Yes	T [61], I [61]	T [61], I [104]
SOR-R-CV(∞)-DFT	∞	No	$U_{ai} = \delta_{ab}\delta_{ij}$	Second	Yes	T [62]	T [62], I [62]
COL-RSCF-CV(∞)-DFT	∞	Yes	$U_{ai} = \delta_{ij}$	Second	Yes	T [104]	T [104], I [104]
SVD-RSCF-CV(∞)-DFT	∞	Yes	$\gamma_1 = 1$	Second	Yes	T [104]	T [104], I [104]

'T' indicates that it is introduced theoretically.
'I' indicates that it is implemented into the code.

Table 1. Variation of CV-DFT applied.

and SVD-RSCF-CV(∞)-DFT. Among the three methods, we have shown that SVD-RSCF-CV (∞)-DFT as rank 1 approximation is the most general form for such a single NTO excitation:

$$\mathbf{U} = v_1^{\sigma\sigma}\left(w_1^{\alpha\alpha}\right)^{\mathrm{T}} \tag{28}$$

where the $v_1^{\sigma\sigma}$ and $w_1^{\alpha\alpha}$ are the vector of the largest singular value $\mathbf{V}^{\sigma\sigma}$ and $\mathbf{W}^{\alpha\alpha}$ out of Eq. (17). The SVD-RSCF-CV(∞)-DFT was also shown to give the same excitation energies as ΔSCF-DFT within 0.1 eV [104].

As a roundup we list the current different versions of CV-DFT in **Table 1**.

3. Applications

In this section, we will show examples of excitations where different versions of CV-DFT have been applied successfully. These excitations are of Rydberg type or possess a dominant charge-transfer character; the work has been published in [99–103]. We would like to note that all CV-DFT-calculations presented here were carried out with developers versions of ADF [112, 113] and we refer to the original publications for the technical details.

3.1. Rydberg excitations

It is well understood that the success of TD-DFT directly depends on how well the approximate exchange-correlation density functional used describes the potential ($\widehat{V}_{XC}^{KS}(\vec{r})$). Further, it is evident that functionals based on the local density approximation (LDA) or the generalized gradient approximation (GGA) result in the potential, $\tilde{V}_{XC}^{KS}(\vec{r})$, that is insufficiently stabilizing

when compared to $\widehat{V}_{XC}^{KS}(\vec{r})$ from an exact functional derived from high-level wave function theory [71–74]. This results in higher occupied orbital ($\tilde{\varepsilon}_i$) and virtual orbital ($\tilde{\varepsilon}_a$) energies obtained with $\tilde{V}_{XC}^{KS}(\vec{r})$ as opposed to those (($\widehat{\varepsilon}_i$),($\widehat{\varepsilon}_a$)) derived from $\widehat{V}_{XC}^{KS}(\vec{r})$. Additionally, the weakness of $\tilde{V}_{XC}^{KS}(\vec{r})$ becomes apparent at medium and large separations r from the polyatomic center of mass where it decays exponentially with r, while $\widehat{V}_{XC}^{KS}(\vec{r})$ decays as $\sim -1/r$.

Excitation energies in TD-DFT are not necessarily affected by the instability of $\tilde{V}_{XC}^{KS}(\vec{r})$ for medium to large values of r in the valence region and in the density tail. This is primarily due to the dependence of the excitation energies in TD-DFT to the difference $\tilde{\varepsilon}_a - \tilde{\varepsilon}_i$. As can be noted, the large errors in the individual orbital energies might be canceled after the energy difference is calculated provided that the average potential experienced by ψ_i and ψ_a shows similar deviations from $\widehat{V}_{XC}^{KS}(\vec{r})$. Resultantly, the success of TD-DFT for valence excitations is attributable to this phenomenon for transitions $\psi_i \rightarrow \psi_a$ where the overlap S_{ia} between the two densities ρ^i and ρ^a is large [92, 114]. However, for cases such as Rydberg transitions [71–74] as well as charge-transfer excitations [77, 79, 82, 90, 96, 97, 115] where S_{ia} is small, the error in $\tilde{V}_{XC}^{KS}(\vec{r})$ gets more pronounced. It is a common practice in the case of small S_{ia} to construct specialized potentials [71–74, 77, 79, 82, 90–98] in which the proper $-1/r$ decay is enforced yielding acceptable results. The disadvantage here is that these parameterized potentials might yield inaccurate results for transitions in which $S_{ia} >> 0$.

Since Rydberg transitions are characterized by a single orbital replacement $\psi_v \rightarrow \psi_r$, RSCF-CV(∞)-DFT will give results very similar to ΔSCF-DFT; this similarity in case of a single NTO transition has been demonstrated in [104]. Although for ΔSCF-DFT, states of the same symmetry as the ground-state almost always decompose to the ground-state, this weakness is absent in RSCF-CV(∞)-DFT. The RSCF-CV(∞)-DFT triplet and singlet transition energies for these single orbital replacement-type excitations are obtained as special case of Eqs. (26) and (27), with the singlet excitation energy given as $2\Delta E_M - \Delta E_T$. In the analysis of Rydberg excitations based on RSCF-CV(∞)-DFT, the excitation energy is considered as a sum of the ionization potential (IP) of a neutral species, A, and the electron affinity (EA) of the resulting cation, A^+, after ionization: $\Delta E(\phi_v \rightarrow \phi_r)$ = EA(A^+, ϕ_v, ϕ_r) + IP(A, ϕ_v). Thus, errors in the excitation energies are due to error in the calculated EAs and IPs. Consequently, a method or 'specialized' *XC* functional that provide accurate EAs and IPs would in turn afford accurate Rydberg excitation energies [100].

Shown in **Table 2** for comparison with the experimental data are the IPs (N_2) and EAs (N_2^+) calculated by RSCF-CV(∞)-DFT (or ΔSCF-DFT). The near-perfect agreement (RMSDs between 0.1 and 0.3 eV) with the experimental data is transferred to the excitation energies afforded by the RSCF-CV(∞)-DFT method. As noted previously by Verma and Bartlett for functionals used within TD-DFT [118–120] and the authors of the work discussed here [100]. A test set including 73 excitations (32 singlet, 41 triplet) from nine different species (N_2, 5; CO, 7; CH_2O, 8; C_2H_2, 8; H_2O, 10; C_2H_4, 13; Be, 6; Mg, 6; Zn, 10) has been used. Broken down into the different species, the results are given in **Table 3** in terms of mean absolute error (MAE) and root-mean-square deviation (RMSD).

Energy term	LDA	BP86	B3LYP	LCBP86*[c]	LCBP86[d]	Expt.
IP(N_2, σ_g)	15.63	15.50	15.74	15.96	16.38	15.58[e,f]
IP(N_2, π_u)	17.46	17.07	16.87	17.22	17.18	17.07[f]
EA(N_2^+, σ_g, $3s\sigma_g$, S)	−3.64	−3.61	−3.49	−3.55	−3.44	−3.38[g]
EA(N_2^+, σ_g, $3p\pi_u$, S)	−2.92	−3.01	−2.87	−2.81	−2.77	−2.68[g]
EA(N_2^+, σ_g, $3p\sigma_u$, S)	−2.84	−2.95	−2.79	−2.71	−2.66	−2.60[g]
EA(N_2^+, π_u, $3s\sigma_g$, S)	−3.77	−3.77	−3.71	−3.73	−3.67	−3.83[g]
EA(N_2^+, σ_g, $3s\sigma_g$, T)	−3.82	−3.81	−3.73	−3.79	−3.72	−3.58[h]

[a]Energies in eV.
[b][72].
[c]Refers to LC functional combined with BP86 and $\omega = 0.40$.
[d]Represents LC functional combined with BP86 and $\omega = 0.75$.
[e][116].
[f][117].
[g]Evaluated as EA(A^+, ϕ_v, ϕ_r, S) = $\Delta E_S(\phi_v \rightarrow \phi_r)$ − IP(A, ϕ_v).
[h]Evaluated as EA(A^+, ϕ_v, ϕ_r, T) = $\Delta E_T(\phi_v \rightarrow \phi_r)$ − IP(A, ϕ_v).
Data represented in this table was first published in [100].

Table 2. IP[a] of N_2 and EA[a] of N_2^+ calculated with ΔSCF using an extended basis set[b] and five different functionals.

Species	No. of states	LDA	BP86	B3LYP	LCBP86*[c]	LCBP86[d]
N_2	5	0.27	0.34	0.05	0.23	0.62
CO	7	0.22	0.43	0.13	0.12	0.37
CH_2O	8	0.21	0.28	0.12	0.20	0.34
C_2H_2	8	0.31	0.50	0.52	0.25	0.24
H_2O	10	0.27	0.17	0.14	0.21	0.24
C_2H_4	13	0.15	0.20	0.28[e]	0.28	0.29
Be	6	0.45	0.60	0.47	0.31	0.23
Mg	6	0.18	0.35	0.19	0.13	0.12
Zn	10	0.18	0.25	0.27	0.34	0.46
RMSD	—	0.24	0.32	0.24	0.23	0.32

[a]Energies in eV.
[b][72].
[c]Refers to LC functional combined with BP86 and $\omega = 0.40$.
[d]Represents LC functional combined with BP86 and $\omega = 0.75$.
[e]Comprising 12 states.
Data represented in this table was first published in [100].

Table 3. Summary of RMSDs of Rydberg excitation energies[a] calculated with ΔSCF using an extended basis set[b] and five different functionals.

The results in **Table 3** for RSCF-CV(∞)-DFT (or ΔSCF-DFT) are in general better than TD-DFT with the same functionals but at par with TD-DFT results with 'specialized' functionals [71–74].

With this benchmark the suitability of RSCF-CV(∞)-DFT without the need for sophisticated (or 'specialized') functionals for Rydberg excitations has been demonstrated. The origin of this good performance is attributable to the ability of RSCF-CV(∞)-DFT to afford good estimates of IPs and EAs for all functionals [100, 121, 122]. Admittedly, fortuitous error cancelation in IPs and EAs obtained for both RSCF-CV(∞)-DFT and TD-DFT plays a role in the accuracy of the resultant excitation energies.

3.2. Charge-transfer excitations

In this subsection we will have a look at excitations with charge-transfer character.

It is well known that TD-DFT applied with standard local exchange and correlation functionals has difficulties for transitions with charge-transfer character between two spatially separated regions [82, 91, 109], a finding nicely explained by Drew, Weisman and Head-Gordon [114]. According to several authors, the reason lies in the exchange and correlation functional [79, 82, 91, 123, 124]. Indeed, a functional like CAM-B3LYP [125] includes a certain Hartree-Fock exchange and results in a clear improvement of TD-DFT excitation energies for transitions involving a charge-transfer character [79, 124, 126]. To further improve the asymptote of the exchange-correlation potential, long-range corrected hybrid scheme like the ones proposed in [76, 95, 98, 127] and asymptotically corrected model potential scheme like in [128, 129] have been designed. Of course modifying the functional is not the only approach, and it is not surprising also that other DFT-based approaches have been suggested, all having their own assets and drawbacks. Several of them have been applied for excitations involving charge-transfer character, for example, constrained orthogonality method (COM) [49, 50], maximum overlap method (MOM) [56], constricted variational density functional theory (CV-DFT) [58] and its extensions [104, 105], constrained density functional theory [130], self-consistent field DFT (ΔSCF-DFT) [131], orthogonality constrained DFT (OCDFT) [63], ensemble DFT [132, 133] and subsystem DFT (FDE-ET) [134].

Ziegler *et al.* showed in [115] how the theoretical framework of CV-DFT is able to cope with excitations including a charge-transfer character and demonstrated this capability with different applications [102, 109, 121]. Here, we will have a look at examples out of three of these mentioned types.

3.2.1. $C_2H_4xC_2F_4$: long-range charge-transfer excitations

Ethylene tetrafluoroethylene, $C_2H_4xC_2F_4$, is a system well studied in literature [76, 91, 93, 114, 126, 134]. It allows for the study of the dependence of excitation energies on the separation of the donor and acceptor and test for the expected $-1/R$ behavior.

For the system $C_2H_4xC_2F_4$, two transitions are of particular interest, the excitations HOMO → LUMO and HOMO-1 → LUMO + 1, both resulting in an excited state of b_1 symmetry. With these transitions, a charge is transferred between the two molecules C_2H_4 and C_2F_4. Although the concrete orbital localization is highly functional dependent, the orbitals HOMO-1, HOMO,

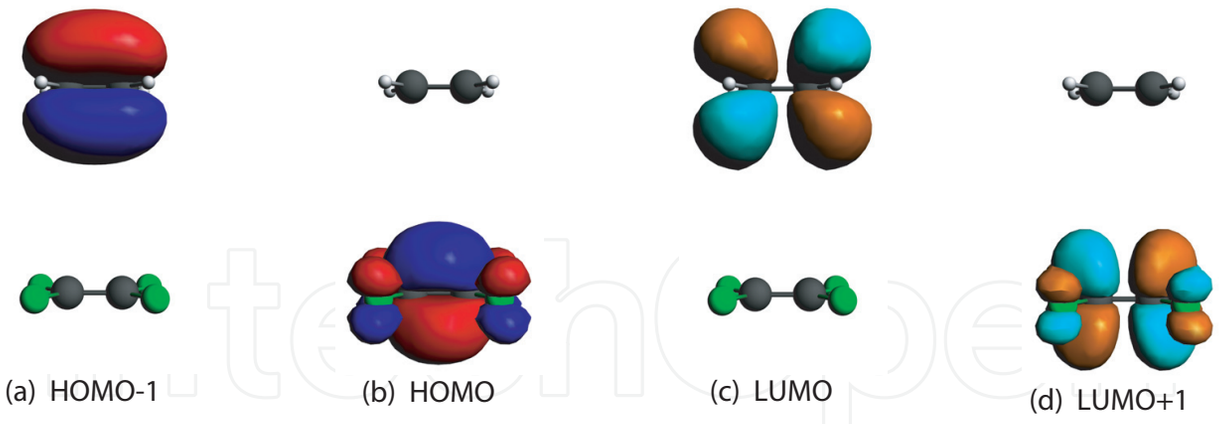

Figure 1. $C_2H_4xC_2F_4$: Representation of ground-state KS orbitals (LDA) ($R = 5.0$ Å) (reprinted from [102], with the permission of AIP Publishing).

LUMO and LUMO + 1 are from certain separation distance, dominantly located on one of the fragments, as visible in **Figure 1** (see, e.g., [77, 102]). It should be noted that for a classification to one of the aforementioned types, it is sufficient when the mentioned ground-state orbitals contribute the most, not necessarily uniquely.

The results obtained with CV-DFT and selected reference values for comparison are shown in **Figure 2**.

First, consideration will be given to the singlet and triplet excitation results with different versions of CV-DFT, where the transition matrix, **U**, is not optimized, before turning to the most general form RSCF-CV(∞)-DFT.

CV(∞)-DFT results in a $-1/R$-like behavior, or when assuming a $\Delta E(R) = -c_1/R + c_0$ function, fitting coefficients c_1 for the results presented in **Figure 2** of 1.1 and 0.9 $E_h a_0$ are obtained. For

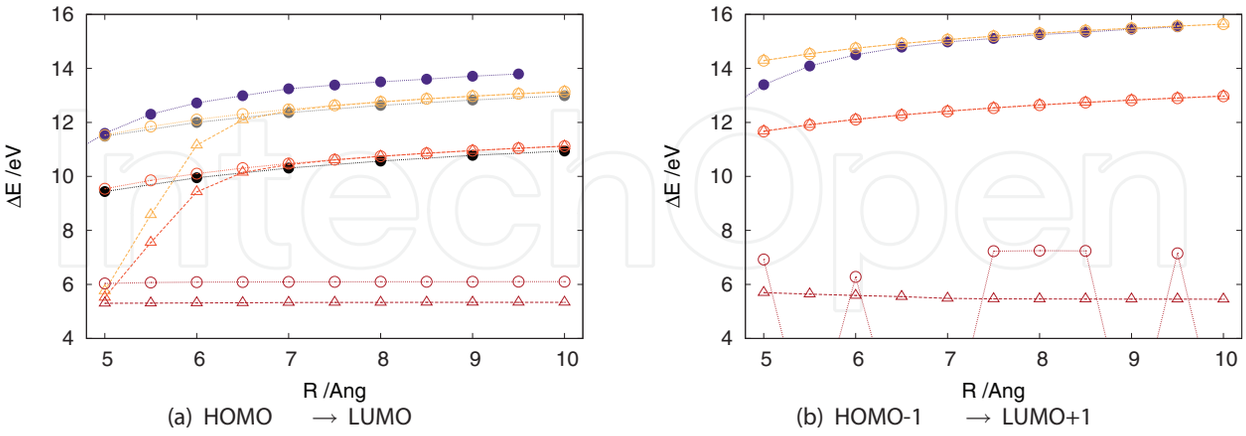

Figure 2. $C_2H_4xC_2F_4$ vertical excitation energies for singlets (circles) and triplets (triangles) using CV(∞)-DFT (orange), R-CV(∞)-DFT (red) and RSCF-CV(∞)-DFT (dark red). The values for the revised hessian out of [96] (purple-filled circles), LC-BLYP out of [76] (black-filled circles) and SAC-CI out of [76] (gray-filled circles) are given as reference. The lines serve as a guide for the eyes, and when the excitation is not dominated by one of the charge-transfer excitations, we set its value to zero (and are therewith not visible in the figure). (reprinted from Senn F, Park YC. The Journal of Chemical Physics. 2016;**145**(24):244108-1 – 10). DOI: 10.1063/1.4972231. with the permission of AIP Publishing. Color specifications refer to the original figure).

these excitations, similar energies are reported using the revised Hessian in [93]. In R-CV(∞)-DFT [61], relaxation of orbitals not directly participating is allowed (see Section 2.3), and it is of no surprise that excitation energies decrease. These results still correspond to a $-1/R$ behavior (resulting in fitting coefficients c_1 for the values presented in **Figure 2** of 1.1 and 0.9 $E_h a_0$). For the HOMO → LUMO transition, the values agree with those reported in [76] using LC-BLYP (MAD = 0.2 eV, RMSD = 0.2 eV). Thus, the extrapolated infinite separation value, $\Delta E_{R\to\infty} =$ 12.7 eV, is close to the $\Delta E_{R\to\infty} = 12.5$ eV reported in [76].

Turning next to the triplet excitations for both CV(∞)-DFT and R-CV(∞)-DFT, similar findings are obtained. At longer distances, no spin interaction is expected; as envisioned the triplet excitation energies match values obtained for the corresponding singlet excitation. Excluding the HOMO → LUMO triplet excitations with $R < 6$ Å, a nice $-1/R$ behavior is obtained.

Until now all the applied methods have one thing in common: the transition matrix **U** has not been optimized. This means the character of the transition itself has not been changed. With CV-DFT being a variational method, the transition matrix **U** can be optimized with the aim of minimizing the energy (see Section 2.3). In this case the RSCF-CV(∞)-DFT method [59–61] is applied, whose strength and merits have been demonstrated several times [100, 104, 121]. From **Figure 2**, it can clearly be seen that RSCF-CV(∞)-DFT minimizes the excitation energy at the expense of nearly distance-independent excitation energies and the loss of the $-1/R$ long-range dependence. This energy gain stems from the optimization of the transition matrix **U**; a thorough explanation is given in [102]. In summary, the charge-transfer transitions, HOMO → LUMO and HOMO-1 → LUMO + 1, are dominated by single NTO transitions. Optimizing the transition matrix results in a mix of (mainly) two NTO transitions with (at least one) different participating fragments, meaning that the two charge-transfer excitations, clearly separated before, do mix now. This mixing of the two different excitations leads to a smaller destabilization and a larger stabilization, resulting in a clear reduction of the excitation energy [102]. An additional issue comes now from having a partial charge $c_A \in (0, 1)$ located on fragment A and a partial charge $1 - c_A$ on fragment B, even when these two fragments are further apart. Therefore, from a certain distance on this mixing should be suppressed. To block the optimization algorithm from mixing such unwanted excitations in RSCF-CV(∞)-DFT calculations, two different strategies have been proposed in [102]. But while working, they both depend highly on an arbitrarily chosen value for a threshold parameter. It remains to be seen, if a strategy without the need of such a parameter can be found for RSCF-CV(∞)-DFT.

3.2.2. Polyacenes: excitations with hidden charge-transfer character

The focus of this subchapter is on polyacenes, a system with an intramolecular charge-transfer-like character, also referred to as charge-transfer in disguise [135]. The polyacenes are understood as a number n_r of linearly fused benzene rings. Such linear polyacenes possess $\pi \to \pi^\star$ excitations L_a (or B_{2u} when the x-axis corresponds to the long molecular axis) and L_b (or B_{3u}) with distinct properties, described, for instance, in [136]. Additionally, these polyacenes have a singlet-triplet gap for which a function of n_r has been proposed. An extrapolation of this function gave rise to a discussion: if polyacenes with a certain size would have a triplet ground state [137–143].

Polyacenes and their derivatives have been used in a plethora of applications; an overview of some of these applications can be found in [144, 145]. Thus, it is not surprising that polyacenes and their excitation energies have been studied extensively. While high-level calculations exist, see, for example, the work presented in [140, 141, 143], considering the size of larger polyacenes TD-DFT calculations is more common. But the latter ones applied with standard functionals have several difficulties. This is why different methods and strategies have been used, each one having its advantages, and we refer to [101] and references therein for more details. Before moving on to the results obtained with CV-DFT, it must be noted that the polyradical character in the ground-state builds up with increasing number of fused acenes, which was deduced by Ibeji *et al.* [143] and was confirmed by Plasser *et al*. [146]. This polyradical character gets bigger and for polyacenes larger than hexacene even big enough to lead to a 'breakdown of single reference approximation used to describe the ground-state of polyacenes in conventional DFT' [132]. Within CV-DFT we rely on a DFT ground-state description. The awareness of this limitation is the reason why only polyacenes as large as hexacene have been studied with CV-DFT.

We will now have a look at the singlet excitation energies. As these energies are not directly measurable, we will use the modified experimental values from Grimme and Parac [136] as reference, for simplicity referred to as experimental results.

As visible from **Table 4** and **Figure 3**, CV(∞)-DFT with LDA results in vertical singlet excitation energies in a very good agreement with the experimental values [147], while for R-CV(∞)-DFT [101], the values deviate more from the experimental ones, although still in an acceptable agreement (a discussion of the difference is given in [101]). As can be seen from **Table 4** and **Figure 3**, both versions of CV-DFT obtain a crossover between 1^1B_{2u} and 1^1B_{3u} for Anthracene onwards, which is in agreement with experimental findings.

No. acene units	Exp.[a]			CV(∞)-DFT[b]			R-CV(∞)-DFT[c]		
	1^1B_{2u}	1^1B_{3u}	ΔE[d]	1^1B_{2u}	1^1B_{3u}	ΔE[d]	1^1B_{2u}	1^1B_{3u}	ΔE[d]
2	4.66	4.13	0.53	4.73	4.39	0.34	4.58	4.42	0.16
3	3.60	3.64	−0.04	3.68	3.73	−0.05	3.46	3.75	−0.29
4	2.88	3.39	−0.51	2.91	3.32	−0.41	2.69	3.33	−0.63
5	2.37	3.12	−0.75	2.35	3.03	−0.68	2.15	3.04	−0.89
6	2.02	2.87	−0.85	1.93	2.82	−0.89	1.74	2.83	−1.09
MAD	—	—	—	0.06	0.11	—	0.18	0.12	
RMSD	—	—	—	0.06	0.13	—	0.19	0.15	

a Out of [136].
b Out of [147].
c Out of [101].
d $\Delta E = \Delta E(1^1B_{2u}) - \Delta E(1^1B_{3u})$.

Table 4. Vertical singlet excitation energies (in eV) for linear polyacenes.

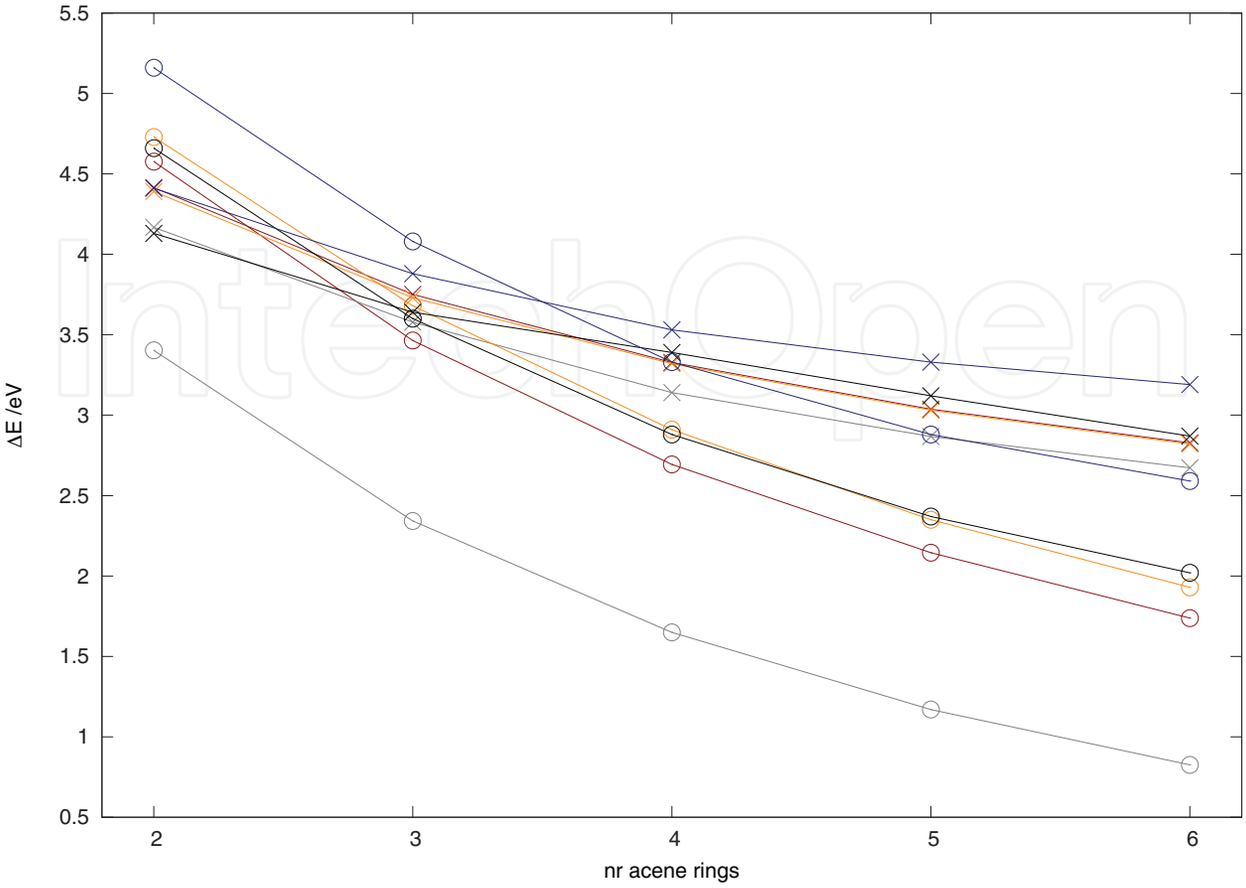

Figure 3. Vertical singlet excitation energies for the states 1^1B_{2u} (circles) and 1^1B_{3u} (crosses) of linear polyacenes: R-CV(∞)-DFT (maroon), *Δ*SCF-DFT (gray), CV-DFT (orange, out of [147]), [143] (dark blue), experimental values (black, out of [136]). The solid lines serve as guides for the eyes. (reprinted with permission from Senn F, Krykunov M. The Journal of Physical Chemistry. A. 2015;**119**(42):10575-10581. DOI: 10.1021/acs.jpca.5b07075. Copyright 2015 American Chemical Society. Color specifications refer to the original figure).

Next, take a look at the obtained triplet excitation energies for the studied polyacenes, shown in **Table 5**. The equivalency of CV(2)-DFT and TD-DFT with the TDA stated in theory section (Section 2.2) is once again confirmed by the numbers in **Table 5**. It can also be seen that in the triplet case, the energies obtained with R-CV(∞)-DFT change only slightly in comparison with the values obtained with CV(2)-DFT, on average by 0.05 eV (for comparison, singlet excitations have a MAD of 0.30 eV for 1^1B_{2u} and 0.13 eV for 1^1B_{3u}, values out of [101, 147]). This surprisingly small difference is due to the nature of the excitation, and for a further discussion of the contributions, we refer to [101].

As previously pointed out in [104], R-CV(∞)-DFT results in triplet states of excitation energies being lower than the ones obtained by coupled cluster methods. Nevertheless, with a RMSD of 0.31 and 0.29 eV, respectively, when compared to the values given in [140 and 143], the results are in reasonable agreement (we note that coordinates were optimized slightly differently). The nature of the triplet excited states is in agreements with the findings of [148], namely, a 1^3B_{2u} state for the first triplet excitation, T_1; for the second triplet excitation, T_2; $^3B_{3u}$ for Naphthalene; and $^3B_{1g}$ for Anthracene to Hexacene.

No. acene units	Vertical					Adiabatic		
	R-CV(∞)-DFT[a]	CV(2)-DFT[a]	TDDFT[b]	Ref. [143]	Ref. [140]	R-CV(∞)-DFT[a]	Exp.[c]	Ref. [143]
2	3.16	3.08	3.08	3.34	3.31	2.89	2.64	2.70
3	2.15	2.09	2.09	2.47	2.47	1.94	1.86	2.06
4	1.49	1.44	1.44	1.82	1.76	1.31	1.27	1.48
5	1.02	0.99	0.99	1.37	1.37	0.88	0.86	1.11
6	0.69	0.66	0.66	1.07	1.00	0.57	0.54	0.83
MAD[d]	—	0.05	0.05	0.31	0.28	—	0.09	0.19
RMSD[d]	—	0.06	0.06	0.32	0.29	—	0.12	0.20

a Out of [101].
b With LDA as functional.
c Out of [143] and references therein.
d To be understood as the deviation of the values obtained with R-CV(∞)-DFT in comparison to the values of this column as reference values.

Table 5. Vertical and adiabatic triplet excitation energies (in eV) for linear polyacenes.

From **Figure 4** one can see the singlet-triplet gap (ST) decreasing, resembling an exponential function. In order to estimate the ST gap for infinitely large polyacenes, giving an indication if there would be a ST crossover, several authors fitted the excitation energies to the function $f(n_r) = a\exp(-b\,n_r) + c$ (see [140, 142, 143]). With the results of R-CV(∞)-DFT for the vertical transition, the limes of an infinitely long polyacene $E^{ST}_{vert}(n_r \to \infty) = (0.3 \pm 4.5)$ kcal mol^{-1} have been obtained and for the 'adiabatic' transition $E^{ST}_{ad}(n_r \to \infty) = (-1.6 \pm 4.0)$ kcal mol^{-1} [101]. For the 'adiabatic' or well-to-well excitations, results from different methods in literature are controversial about a possible ST gap crossover ([140, 142] versus [143, 149, 150]); for TD-DFT it even depends on the functional used [142]. Therefore, necessarily the findings presented here will agree with some findings, while disagree with others. It should be noted that these energies are very small, actually smaller than the estimated accuracy of the CV-DFT method, and with its error it must be regarded as giving only a tendency for no ST crossover. Two additional points of precaution which puts the value of the extrapolated results into question: (a) it has been shown in [142] how a small change of a single excitation energy can influence the obtained polymeric limit, and (b) one should have in mind the change of the ground-state character with the polyacene length and, thus, the number of fused acenes.

3.2.3. Charge-transfer excitations in transition metals

The complicated electronic structure of transition metal (TM) complexes [151] makes them ideal for testing the performance of newly developed methods. This section deals with charge-transfer (and hidden charge-transfer) excitations in these complexes, more precisely the 3d complexes MnO_4^-, CrO_4^{2-} and VO_4^{3-}, as well as their 4d congeners RuO_4, TcO_4^-, MoO_4^{2-} and 5d homologues OsO_4, ReO_4^- and WO_4^{2-} [99]. For these systems, the three lowest valence excitations involving transitions from $1t_1$, $2t_2$ to $2e$ and $3t_2$ are considered [99]. The comparison is

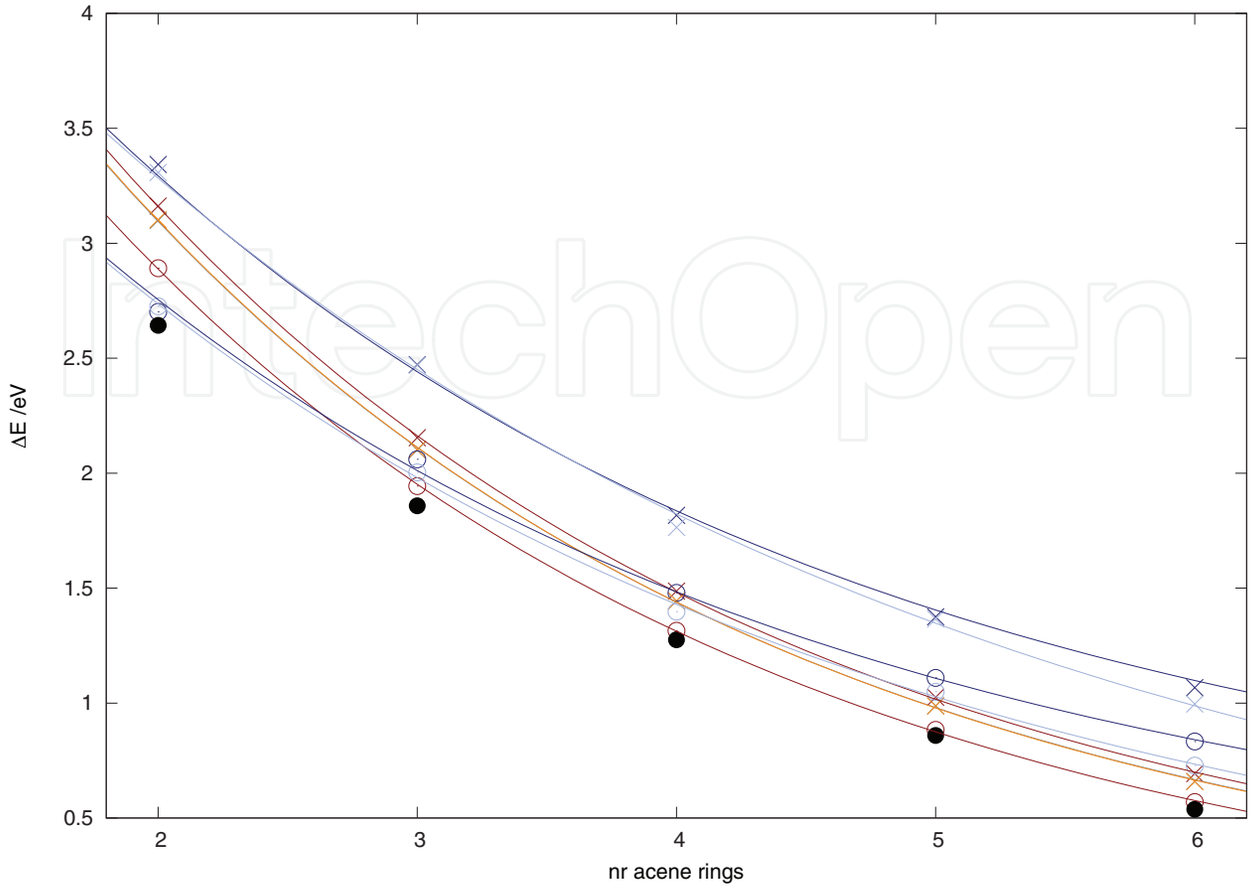

Figure 4. Triplet excitation energies for the 1^3B_{2u} states of linear polyacenes: R-CV(∞)-DFT (maroon), ΔSCF-DFT (gray), SVD-R-CV(∞)-DFT (orange), [143] (dark blue), [140] (light blue), experimental values (black, out of [143] and references therein). The symbols are used to distinguish between vertical transitions (crosses) and adiabatic as well as 'imitated adiabatic' transitions (circles). The lines are the curves fitted to the function $f(n_r) = a \exp(-b n_r) + c$ and serve as guides for the eyes. (reprinted with permission from Senn F, Krykunov M. The Journal of Physical Chemistry. A. 2015;**119**(42):10575-10581. DOI: 10.1021/acs.jpca.5b07075. Copyright 2015 American Chemical Society. Color specifications refer to the original figure).

made with available experimental data [152, 153] and high-level *ab initio* calculations [154–160]. There are several adjustable parameters that can influence the excitation energies. These include the size of the basis set used, functionals used, geometry (optimized structures or experimental geometries), medium (since the complexes are anions), etc. Use was made of experimental structures which lead to higher excitation energies (0.1–0.3 eV) compared to optimized structures. Marginal influence of solvation was found for the three valence excitations; the calculated COSMO [161, 162] excitation energies lower the energies by 0.01–0.02 eV [163, 164].

Table 6 displays the RMSD between the first three experimental dipole-allowed transitions and the corresponding values calculated by RSCF-CV(∞)-DFT.

On average, the three functionals B3LYP, PBE0 with an intermediate fraction of HF exchange and LCBP86* have the lowest RMSD of 0.2 eV, whereas the local functionals (LDA, BP86, BPE) and BHLYP with the highest HF fraction and LCBP86 have a somewhat larger RMSD of 0.3 eV for both 3d and 4d + 5d averages. TD-DFT with the same functionals performs poorly for the 3d complexes but shows good agreement with experiment for the heavier tetraoxo complexes.

Complex	LDA	BP86	PBE	B3LYP	BHLYP	PBE0	LCBP86*	LCBP86
MnO^-_4	0.41	0.32	0.33	0.15	0.62	0.19	0.24	0.37
CrO_4^{2-}	0.40	0.31	0.34	0.09	0.55	0.04	0.22	0.32
VO_4^{3-}	0.25	0.14	0.16	0.07	0.18	0.14	0.27	0.37
RuO_4	0.32	0.28	0.28	0.21	0.44	0.22	0.19	0.31
TcO^-_4	0.10	0.13	0.13	0.25	0.13	0.29	0.27	0.17
MoO_4^{2-}	0.14	0.23	0.23	0.06	0.22	0.18	0.13	0.34
OsO_4	0.53	0.51	0.50	0.27	0.39	0.31	0.21	0.26
ReO^-_4	0.36	0.43	0.43	0.14	0.25	0.16	0.14	0.16
WO_4^{2-}	0.43	0.51	0.51	0.14	0.11	0.07	0.11	0.16
Average 3d[f]	0.35	0.26	0.28	0.10	0.45	0.12	0.24	0.35
Average 4d + 5d[g]	0.31	0.34	0.34	0.19	0.27	0.22	0.19	0.24
Total average 3d[h]	0.33	0.31	0.32	0.16	0.34	0.18	0.21	0.28

[a]Root-mean-square deviation.
[b]The reference is the observed vertical excitation energies for the three first dipole-allowed transitions.
[c]For MoO_4^{2-} and WO_4^{2-} only, the first two experimental transitions are available.
[d]Deviations are in eV.
[e]No TDA was applied.
[f]Average of the three 3d complexes.
[g]Average of the six 4d and 5d complexes.
[h]Average over all complexes.
Data represented in this table was first published in [99].

Table 6. RMSDs for tetraoxo excitation energies based on RSCF-CV(∞)-DFT and a TZ2P basis set[a, b, c, d, e].

This shows a clear lack of consistency. However, RSCF-CV(∞)-DFT shows good and consistent performance for all complexes studied here.

Next, the excitation energies of the octahedral TM complexes [103] are presented. The analyses will be primarily focused on $Cr(CO)_6$ and $[Fe(CN)_6]^{4-}$ where experimental excitation energies are available. The first system to be considered is $Cr(CO)_6$; the RSCF-CV(∞)-DFT results are displayed in **Table 7**. The results afforded by RSCF-CV(∞)-DFT are in good agreement with the experimental data even at the RSCF-CV(∞)-DFT/LDA level of theory. The RSCF-CV(∞)-DFT/LDA results show performance identical to the TD-DFT/B3LYP [151] and better performance than TD-DFT with LDA and GGAs.

Considered next is the $[Fe(CN)_6]^{4-}$ complex; the results are shown in **Table 8**. The RMSDs here were calculated with the lower limit of the experimental [153] excitation energies where ranges are applicable. There are some theoretical calculations carried with TD-DFT [151] and other DFT-based approaches [151] as well as some high-level *ab initio* methods [156]. Again, there are good performances even for the LDA and GGA functionals. The accurate excitation energies afforded by the RSCF-CV(∞)-DFT method when compared to the experimental data are as a result of, to some extent, fortuitous error cancelation.

STATE	RASPT2[b]	LDA	BP86	PBE	B3LYP	PBE0	BHLYP	LCBP86*[c]	LCBP86[d]	Expt.[e]
Singlet										
$^1T_{1g}$(MC)	4.98	5.33	5.14	5.17	4.85	5.25	4.52	4.78	4.97	—
$^1T_{1u}$(MLCT)	4.50	4.45	4.39	4.40	4.48	4.62	4.68	4.61	4.37	4.44
2^1T_{1u}(MLCT)	5.42	5.46	5.47	5.47	5.73	5.93	6.20	6.23	5.85	5.48
Triplet										
1^3T_{1g}(MC)	4.28[f]	4.72	4.88	4.91	4.54	4.62	4.15	4.18	4.49	—
1^3T_{2g}(MC)	4.64[f]	4.63	4.59	4.60	4.39	4.45	4.17	4.45	4.59	—
RMSD	0.06	0.02	0.04	0.03	0.18	0.34	0.54	0.54	0.27	

[a]Energies in eV.
[b][154].
[c]Represents LC functional combined with BP86 with $\omega = 0.75$.
[d]Refers to LC functional combined with BP86 using $\omega = 0.4$.
[e][152].
[f][155].
Data represented in this table was first published in [103].

Table 7. Calculated excitation energies[a] for $Cr(CO)_6$ based on the RSCF-CV(∞)-DFT method.

STATE	CASPT2[b]	LDA	BP86	PBE	B3LYP	PBE0	BHLYP	LCBP86*[c]	LCBP86[d]	Expt.[e]
Singlet										
$^1T_{1g}$(MC)	3.60	4.17	3.72	3.75	3.42	3.35	3.04	3.35	3.64	3.80–3.94
3^1T_{1u}(MLCT)	—	5.57	5.57	5.64	6.10	6.44	—	—	6.34	5.69–5.89
4^1T_{1u}(MLCT)	—	5.83	5.80	5.72	6.25	6.63	—	—	6.93	6.20
1^1T_{2g}(MC)	4.33	4.05	3.74	4.12	4.47	4.46	4.47	4.14	4.37	4.43–4.77
Triplet										
1^3T_{1g}(MC)	2.67	3.60	3.39	3.41	2.98	2.90	2.49	2.56	2.93	2.94
RMSD	0.20[f]	0.42	0.41	0.33	0.25	0.44	0.40[f]	0.29[f]	0.44	

[a]Energies in eV.
[b][156].
[c]Represents LC functional combined with BP86 with $\omega = 0.75$.
[d]Refers to LC functional combined with BP86 using $\omega = 0.4$.
[e][153].
[f]Calculated with three excitation energies.
Data represented in this table was first published in [103].

Table 8. Calculated excitation energies[a] for $[Fe(CN)_6]^{4-}$ based on the RSCF-CV(∞)-DFT method.

A look now at the electronic density change that accompanies the electronic excitation. **Figure 5** (**a** and **b**) shows the plot of the density changes associated with the electronic transitions in Cr $(CO)_6$. The charge redistribution can be seen from the figure, where the density depletion (ρ_{occ}), the accumulation (ρ_{vir}) as well as the density change ($\Delta\rho_{ex} = \rho_{vir} - \rho_{occ}$) occurs, resulting from the total change in density associated with the electronic transition. For the MLCT transition, the ρ_{occ} (**Figure 5a**) is situated on the Cr metal center, the area or space spun by the density that is reminiscent of the d_{yz} and the ρ_{vir} is mostly situated on the equatorial CO ligands. The depletion density is in the yz plane, the accumulation density is situated on the CO ligand, and there is little interaction between them as can be seen from the difference (**Figure 5b**). The movement of density is from the metal center to the ligands corresponding to an intramolecular charge-transfer transition. It is clear from **Figure 5c** that this transition has a significant $d \rightarrow d$ character. In the density plots that follow, there is a depletion in the density situated on

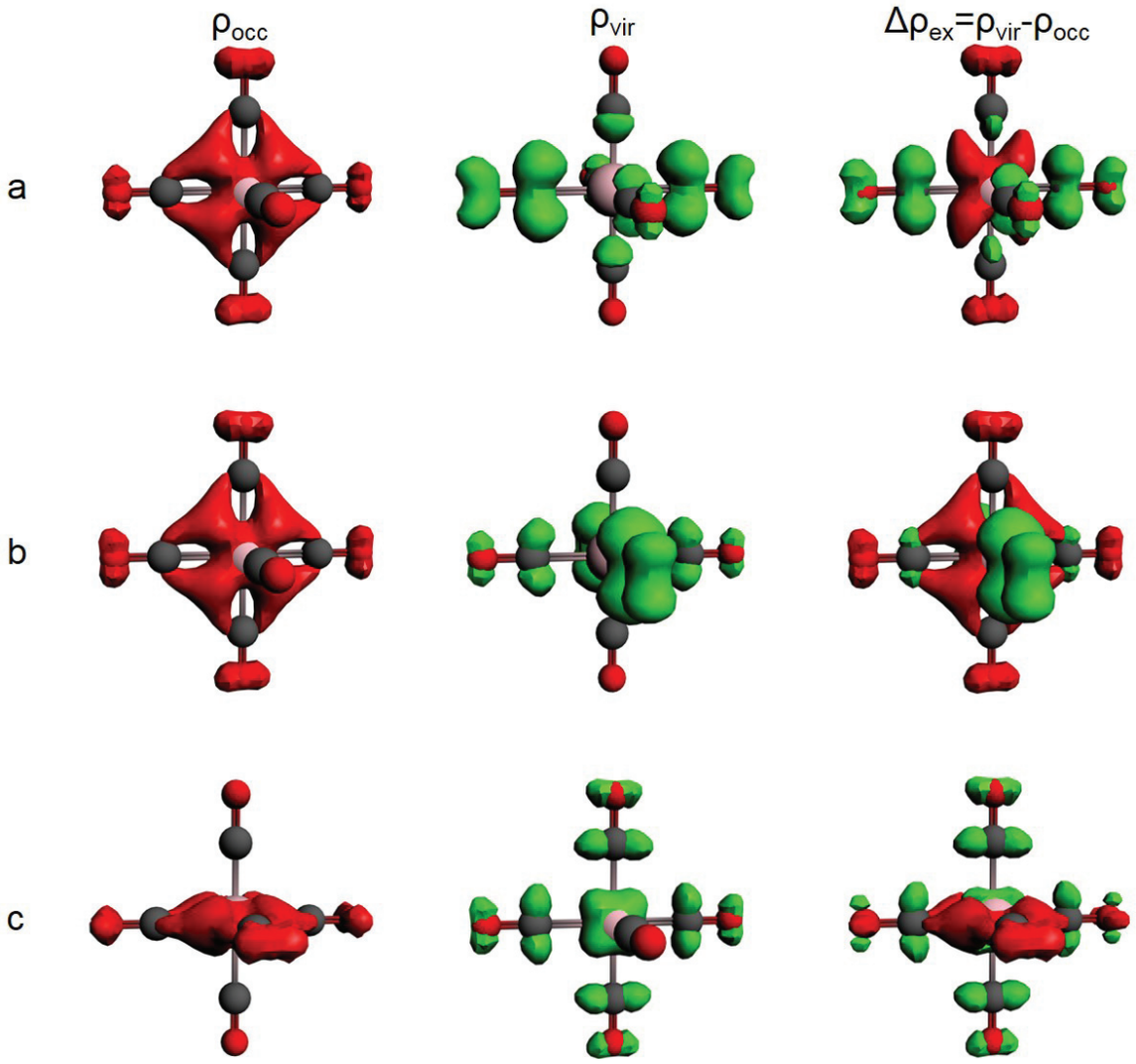

Figure 5. Δρ associated with the $CrCO_6$, red signifies depletion and green shows accumulation of density. (a) The density change associated with the 1^1T_{1u} state. (b) Exemplifies the density redistribution associated with the 2^1T_{1u} state. (c) Densities accompanying the calculated 1^1T_{1g} state. (a) and (b) are MLCT-type transitions, and (c) is an example of MC-type transition. See Seidu I. Excited-State Studies with the Constricted Variational Density Functional Theory (CV-DFT) Method. PhD dissertation. University of Calgary; 2016 for coloured pictures.

http://dx.doi.org/10.5772/intechopen.70932

the metal with some contribution from the CO in the *xy*-plane and accumulation of density largely on the central Cr metal along the *yz*-plane with some accumulation on the CO ligands in the same plane.

Displayed in **Figure 6** are the density plots for $[Fe(CN)_6]^{4-}$. Similar features are seen here as seen for $Cr(CO)_6$. The differences in the density plots representing the MC transition; there is more significant accumulation on the CN^- ligands, and the density accumulation is in the same plane (*xy*-plane) as the depletion density ($d_{x^2-y^2}$–d_{xy}). As for the MLCT, the associated density movement is identical to that of $Cr(CO)_6$ (see **Figure 6**(**b** and **c**)).

The benchmark studies on the tetrahedral and octahedral TM complexes probed the ability of RSCF-CV(∞)-DFT to describe CT and hidden CT excitations. Use was made of the tetrahedral d^0 metal oxides as the first benchmark series since the tetra oxides have a long history as a

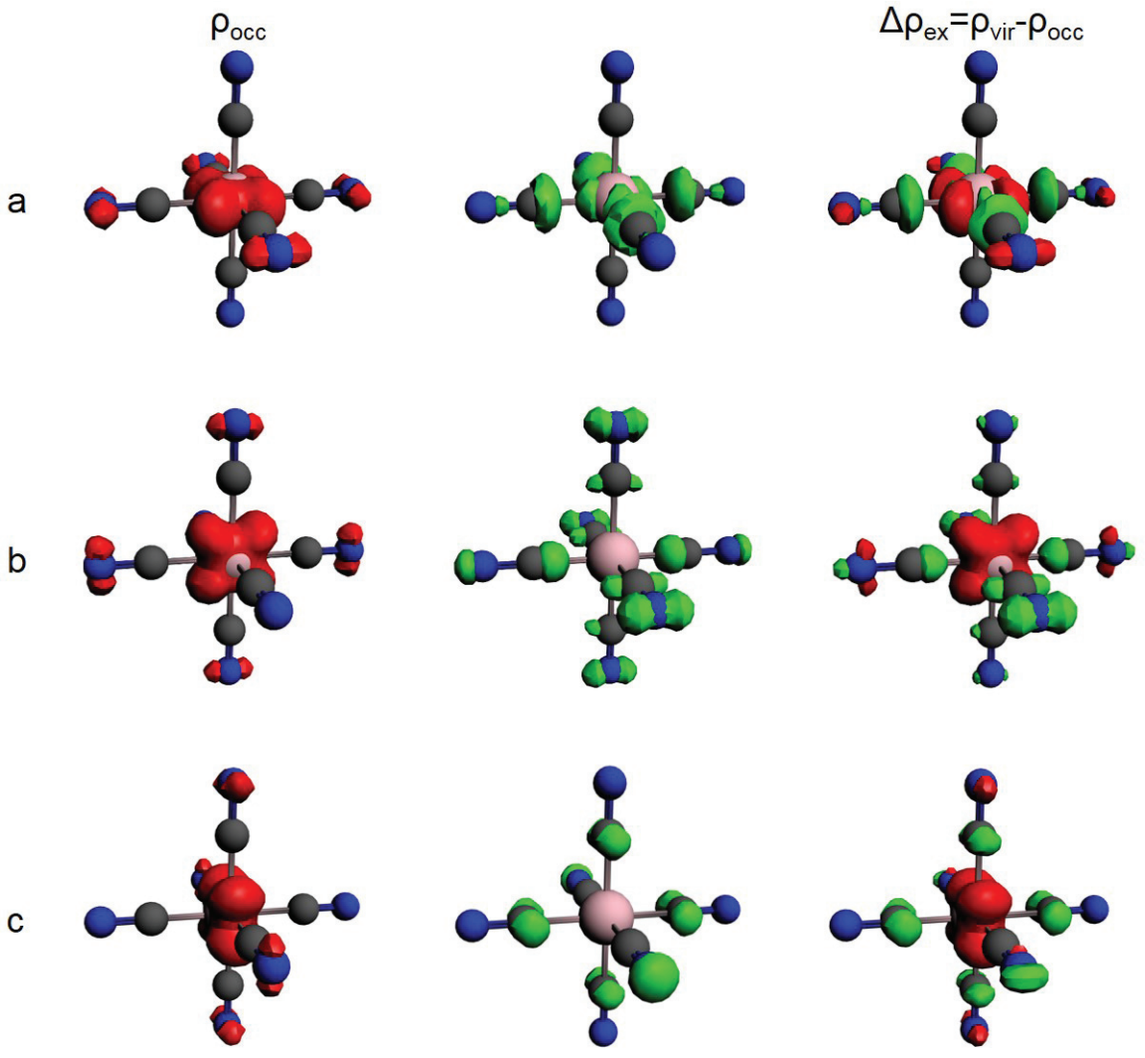

Figure 6. $\Delta\rho$ associated with the $Fe(CN)_6^{4-}$. (a) the density change associated with the 1^1T_{1g} state. (b) Exemplifies the density redistribution associated with the 3^1T_{1u} state. (c) Densities accompanying the calculated 3^1T_{1u} state. (a) Is an example of MC-type transition, and (b) and (c) are MLCT-type transitions. Red signifies loss and green shows gain in density. See Seidu I. Excited-State Studies with the Constricted Variational Density Functional Theory (CV-DFT) Method. PhD dissertation. University of Calgary; 2016 for coloured pictures.

challenging testing ground for new methods due to their complex electronic structure. In general there is either a comparable performance for RSCF-CV(∞)-DFT and TD-DFT in cases where TD-DFT shows good performances or RSCF-CV(∞)-DFT outperforms TD-DFT.

A trend that manifests itself at larger r for the TM complexes is the excitation energies which become more functional dependent and less accurate. Further, the accuracy of RSCF-CV(∞)-DFT for smaller r is not attributable to the ability of our method to afford accurate values of the IP of the complex and the EA of the cation formed alone; some error cancelation occurs when the IPs and EAs are combined to obtain the excitation energy. Finally, it is possible to plot the density change associated with the electronic transitions afforded by our method with regions of density depletion and accumulation supporting a qualitative classification of excitations as MLCT or MC.

4. Conclusion

In this chapter we presented the CV-DFT method and its different variants. While CV(2)-DFT is consistent with (adiabatic) TD-DFT within the TDA approximation, CV-DFT allows to go to higher order. Indeed, its strength lies in going beyond linear response and therewith obtaining distance-dependent contributions to the excitation energy naturally. Additionally, the theory allows for the calculation of excitation energies for singlet and triplet states on the same footing. Of course as a variational method, CV-DFT relies on an accurate ground-state description. The theoretical framework allows us to apply special restrictions as done in [104] and therewith obtain a numerically stable method being numerically equivalent to ΔSCF-DFT.

How CV-DFT performs has been shown in Section 3 with the aid of selected examples of charge-transfer or Rydberg excitation type. With these examples, we could demonstrate how CV(∞)-DFT is able to reproduce the expected $-1/R$ long-range behavior for charge-transfer excitations. When orbital relaxation is allowed, the excitation energies obtained by R-CV(∞)-DFT with LDA agree nicely with the findings of long-range corrected functionals. For short distance, the optimization of the transition matrix **U** is clearly beneficial [100, 104, 121]. But for medium- and long-range distances, a notion of care is to be taken as the optimization may lead to an unwanted mixing of transitions as shown in the case of $C_2H_4xC_2F_4$. Also, for excitations with hidden charge-transfer character, meaningful results are obtained with CV-DFT, for example, accurate results for the first singlet excitation energies of polyacenes [101, 147] for polyacenes as large as hexacene. Not only is CV-DFT able to deliver meaningful results, even for the LDA functional, it has an incredible ability to provide a qualitative picture of the nature or type of excitation under consideration. This is seen in the case of the TM complexes, a complicated yet excellent test set for assessing the range of applicability of every newly developed method. In the case of Rydberg excitations, RSCF-CV(∞)-DFT produces meaningful results without the need for sophisticated (or 'specialized') functionals. This good performance is attributable to the ability of our method affords good estimates of IPs and EAs for all functionals [100, 121, 122]. Admittedly, fortuitous error cancelation in IPs and EAs obtained for both RSCF-CV(∞)-DFT and TD-DFT plays a role in the accuracy of the resultant excitation energies.

Acknowledgements

The authors would like to express their gratitude to the late Prof. Dr. Tom Ziegler for his unflinching support until his untimely passing away.

Further, the authors are grateful to Dr. Mykhaylo Krykunov for his helpful discussions.

Author details

Florian Senn[1]*, Issaka Seidu[2] and Young Choon Park[3]

*Address all correspondence to: florian.senn@ucalgary.ca

1 Department of Chemistry, University of Calgary, Calgary, Alberta, Canada

2 Department of Chemistry, Carleton University, Ottawa, Ontario, Canada

3 Quantum Theory Project, University of Florida, Gainesville, FL, United States

References

[1] Wolfsberg M, Helmholz L. The Journal of Chemical Physics. 1952;**20**(5):837-843. DOI: http://dx.doi.org/10.1063/1.1700580

[2] Hoffmann R. The Journal of Chemical Physics. 1963;**39**(6):1397-1412. DOI: http://dx.doi.org/10.1063/1.1734456

[3] Pople JA, Santry DP, Segal GA. The Journal of Chemical Physics. 1965;**43**(10):S129-S135. DOI: http://dx.doi.org/10.1063/1.1701475

[4] Holt S, Ballhausen C. Theoretica Chimica Acta. 1967;**7**(4):313-320. DOI: 10.1007/BF00537508

[5] Hillier H, Saunders VR. Proceedings of the Royal Society of London, Series A. 1970; **320**(1541):161-173. DOI: 10.1098/rspa.1970.0203

[6] Slater JC. In: Löwdin PO, editor. Advances in Quantum Chemistry, Vol. 6 of *Advances in Quantum Chemistry*: 1-92. Academic Press; 1972. DOI: http://dx.doi.org/10.1016/S0065-3276(08)60541-9

[7] Hall MB, Fenske RF. Inorganic Chemistry. 1972;**11**(4):768-775. DOI: 10.1021/ic50110a022

[8] Truax DR, Geer JA, Ziegler T. The Journal of Chemical Physics. 1973;**59**(12):6662-6666. DOI: http://dx.doi.org/10.1063/1.1680049

[9] Ziegler T, Rauk A, Baerends E. Theoretica Chimica Acta. 1977;**43**(3):261-271. DOI: 10.1007/BF00551551

[10] Dewar MJS, Thiel W. Journal of the American Chemical Society. 1977;**99**(15):4899-4907. DOI: 10.1021/ja00457a004

[11] Hall MB. Journal of the American Chemical Society. 1978;**100**(20):6333-6338. DOI: 10.1021/ja00488a007

[12] Stewart JJP. Journal of Computational Chemistry. 1989;**10**(2):221-264. DOI: 10.1002/jcc.540100209

[13] Bursten BE, Drummond ML, Li J. Faraday Discussions. 2003;**124**:1-24. DOI: 10.1039/B305317M

[14] Buenker RJ, Peyerimhoff SD. Theoretica Chimica Acta. 1968;**12**(3):183-199. DOI: 10.1007/BF00528266

[15] Levy B, Berthier G. International Journal of Quantum Chemistry. 1969;**3**(2):247-247. DOI: 10.1002/qua.560030213

[16] Godefroid M, Lievin J, Metz JY. International Journal of Quantum Chemistry. 1991;**40**(2):243-264. DOI: 10.1002/qua.560400207

[17] Hegarty D, Robb MA. Molecular Physics. 1979;**38**(6):1795-1812. DOI: 10.1080/00268977900102871

[18] Maruhn-Rezwani V, Grün N, Scheid W. Physical Review Letters. 1979;**43**:512-515. DOI: 10.1103/PhysRevLett.43.512

[19] Kulander KC, Devi KRS, Koonin SE. Physical Review A. 1982;**25**:2968-2975. DOI: 10.1103/PhysRevA.25.2968

[20] Devi KRS, Garcia JD. Physical Review A. 1984;**30**:600-603. DOI: 10.1103/PhysRevA.30.600

[21] Kulander KC. Physical Review A. 1987;**36**:2726-2738. DOI: 10.1103/PhysRevA.36.2726

[22] Olsen J, Roos BO, Jørgensen P, Jensen HJA. The Journal of Chemical Physics. 1988;**89**(4):2185-2192. DOI: http://dx.doi.org/10.1063/1.455063

[23] Malmqvist PÅ, Pierloot K, Shahi ARM, Cramer CJ, Gagliardi L. The Journal of Chemical Physics. 2008;**128**(20):204109. DOI: http://dx.doi.org/10.1063/1.2920188

[24] Andersson K, Malmqvist PÅ, Roos BO. The Journal of Chemical Physics. 1992;**96**(2):1218-1226. DOI: http://dx.doi.org/10.1063/1.462209

[25] Stanton JF, Bartlett RJ. The Journal of Chemical Physics. 1993;**98**(9):7029-7039. DOI: http://dx.doi.org/10.1063/1.464746

[26] Angeli C, Cimiraglia R, Evangelisti S, Leininger T, Malrieu JP. The Journal of Chemical Physics. 2001;**114**(23):10252-10264. DOI: http://dx.doi.org/10.1063/1.1361246

[27] Neese F. The Journal of Chemical Physics. 2003;**119**(18):9428-9443. DOI: http://dx.doi.org/10.1063/1.1615956

[28] Crawford TD, Schaefer HF. An Introduction to Coupled Cluster Theory for Computational Chemists. John Wiley & Sons, Inc.; 2007. pp. 33-136. DOI: 10.1002/9780470125915.ch2

[29] Bartlett RJ, Stanton JF. Applications of Post-Hartree-Fock Methods: A Tutorial. John Wiley & Sons, Inc.; 2007. pp. 65-169. DOI: 10.1002/9780470125823.ch2

[30] Kohn W, Sham LJ. Physics Review. 1965;**140**:A1133-A1138. DOI: 10.1103/PhysRev.140.A1133

[31] Slater JC. Physics Review. 1951;**81**(3):385-390. DOI: 10.1103/PhysRev.81.385

[32] Slater JC, Wood JH. International Journal of Quantum Chemistry. 1970;**5**(S4):3-34. DOI: 10.1002/qua.560050703

[33] Slater JC. Advances in Quantum Chemistry, 1972;**6**:1-92. Academic Press; DOI: http://dx.doi.org/10.1016/S0065-3276(08)60541-9

[34] Nagy Á. Physical Review A. 1996;**53**(5):3660-3663. DOI: 10.1103/PhysRevA.53.3660

[35] Liu T, Han WG, Himo F, Ullmann GM, Bashford D, et al. The Journal of Physical Chemistry. A. 2004;**108**(16):3545-3555. DOI: 10.1021/jp031062p

[36] Gavnholt J, Olsen T, Engelund M, Schiotz J. Physical Review B: Condensed Matter and Materials Physics. 2008;**78**(7):075441–1 – 10. DOI: 10.1103/PhysRevB.78.075441

[37] Theophilou AK. Journal of Physics C: Solid State Physics. 1979;**12**(24):5419-5430

[38] Gross EKU, Oliveira LN, Kohn W. Physical Review A. 1988;**37**:2821-2833. DOI: 10.1103/PhysRevA.37.2809

[39] Gidopoulos N, Papaconstantinou P, Gross EKU. Physical Review Letters. 2002;**88**(3):033003–1 – 4. DOI: 10.1103/PhysRevLett.88.033003

[40] Casida ME. Time-Dependent Density Functional Response Theory for Molecules, Chap. 5. World Scientific; 1995. pp. 155-192. DOI: 10.1142/9789812830586_0005

[41] Runge E, Gross EKU. Physical Review Letters. 1984;**52**(12):997-1000. DOI: 10.1103/PhysRevLett.52.997

[42] Casida ME. The Journal of Chemical Physics. 2005;**122**(5):054111. DOI: http://dx.doi.org/10.1063/1.1836757

[43] Casida M, Huix-Rotllant M. In: Ferré N, Filatov M, Huix-Rotllant M, editors. Density-Functional Methods for Excited States, vol. 368 of Top. Curr. Chem., 1-60. Springer International Publishing, 2016; DOI: 10.1007/128_2015_632

[44] Casida ME, Jamorski C, Casida KC, Salahub DR. The Journal of Chemical Physics. 1998;**108**(11):4439-4449. DOI: http://dx.doi.org/10.1063/1.475855

[45] Oliveira L, Gross EKU, Kohn W. Physical Review A. 1988;**37**(8):2821-2833. DOI: 10.1103/PhysRevA.37.2821

[46] Filatov M, Shaik S. Chemical Physics Letters. 1998;**288**(5–6):689-697

[47] Filatov M, Shaik S. Chemical Physics Letters, 1999;**304**(5–6):429-437. DOI: http://dx.doi.org/10.1016/S0009-2614(99)00336-X

[48] Pederson MR, Klein BM. Physical Review B. 1988;**37**:10319-10331. DOI: 10.1103/PhysRevB.37.10319

[49] Baruah T, Pederson MR. The Journal of Chemical Physics. 2006;**125**(16):164706. DOI: http://dx.doi.org/10.1063/1.2360265

[50] Baruah T, Pederson MR. Journal of Chemical Theory and Computation. 2009;**5**(4):834-843. DOI: 10.1021/ct900024f

[51] Frank I, Hutter J, Marx D, Parrinello M. The Journal of Chemical Physics. 1998;**108**(10):4060-4069. DOI: http://dx.doi.org/10.1063/1.475804

[52] Okazaki I, Sato F, Yoshihiro T, Ueno T, Kashiwagi H. THEOCHEM Journal of Molecular Structure. 1998;**451**(1–2):109-119. DOI: http://dx.doi.org/10.1016/S0166-1280(98)00164-X

[53] Wu Q, Van Voorhis T. Physical Review A. 2005;**72**:024502–1–4. DOI: 10.1103/PhysRevA.72.024502

[54] Glushkov VN, Levy M. The Journal of Chemical Physics. 2007;**126**(17):174106. DOI: http://dx.doi.org/10.1063/1.2733657

[55] Glushkov VN, Assfeld X. The Journal of Chemical Physics. 2010;**132**(20):204106. DOI: http://dx.doi.org/10.1063/1.3443777

[56] Gilbert ATB, Besley NA, Gill PMW. The Journal of Physical Chemistry. A. 2008;**112**(50):13164-13171. DOI: 10.1021/jp801738f

[57] Besley NA, Gilbert ATB, Gill PMW. The Journal of Chemical Physics. 2009;**130**(12) 124308–1 – 7. DOI: http://dx.doi.org/10.1063/1.3092928

[58] Ziegler T, Seth M, Krykunov M, Autschbach J, Wang F. The Journal of Chemical Physics. 2009;**130**(15):154102. DOI: http://dx.doi.org/10.1063/1.3114988

[59] Cullen J, Krykunov M, Ziegler T. Chemical Physics. 2011;**391**(1):11-18. DOI: http://dx.doi.org/10.1016/j.chemphys.2011.05.021

[60] Ziegler T, Krykunov M, Cullen J. The Journal of Chemical Physics. 2012;**136**(12):124107. DOI: http://dx.doi.org/10.1063/1.3696967

[61] Krykunov M, Ziegler T. Journal of Chemical Theory and Computation. 2013;**9**(6):2761-2773. DOI: 10.1021/ct300891k

[62] Park YC, Krykunov M, Ziegler T. Molecular Physics. 2015;**113**(13–14):1636-1647. DOI: 10.1080/00268976.2014.1003260

[63] Evangelista FA, Shushkov P, Tully JC. The Journal of Physical Chemistry. A. 2013;**117**(32):7378-7392. DOI: 10.1021/jp401323d

[64] Peng B, Van Kuiken BE, Ding F, Li X. Journal of Chemical Theory and Computation. 2013;**9**(9):3933-3938. DOI: 10.1021/ct400547n

[65] van Gisbergen SJA, Snijders JG, Baerends EJ. The Journal of Chemical Physics. 1995; **103**(21):9347-9354. DOI: http://dx.doi.org/10.1063/1.469994

[66] Petersilka M, Gossmann U, Gross EKU. Physical Review Letters. 1996;**76**(8):1212-1215. DOI: 10.1103/PhysRevLett.76.1212

[67] Bauernschmitt R, Ahlrichs R. Chemical Physics Letters. 1996;**256**(4):454-464. DOI: http://dx.doi.org/10.1016/0009-2614(96)00440-X

[68] Furche F. The Journal of Chemical Physics. 2001;**114**(14):5982-5992. DOI: http://dx.doi.org/10.1063/1.1353585

[69] Furche F, Ahlrichs R. The Journal of Chemical Physics. 2002;**117**(16):7433-7447. DOI: http://dx.doi.org/10.1063/1.1508368

[70] Ullrich CA. Time-Dependent Density-Functional Theory. Oxford Graduate Texts, 2012

[71] Tozer DJ, Handy NC. The Journal of Chemical Physics. 1998;**109**(23):10180-10189. DOI: http://dx.doi.org/10.1063/1.477711

[72] Schipper PRT, Gritsenko OV, van Gisbergen SJA, Baerends EJ. The Journal of Chemical Physics, 2000;**112**(3):1344-1352. DOI: http://dx.doi.org/10.1063/1.480688

[73] Wasserman A, Burke K. Physical Review Letters. 2005;**95**:163006–1 – 4. DOI: 10.1103/PhysRevLett.95.163006

[74] Gaiduk AP, Firaha DS, Staroverov VN. Physical Review Letters. 2012;**108**:253005–1 – 5. DOI: 10.1103/PhysRevLett.108.253005

[75] Jaramillo J, Scuseria GE, Ernzerhof M. The Journal of Chemical Physics. 2003; **118**(3):1068-1073. DOI: http://dx.doi.org/10.1063/1.1528936

[76] Tawada Y, Tsuneda T, Yanagisawa S, Yanai T, Hirao K. The Journal of Chemical Physics. 2004;**120**(18):8425-8433. DOI: http://dx.doi.org/10.1063/1.1688752

[77] Neugebauer J, Gritsenko O, Baerends EJ. The Journal of Chemical Physics. 2006; **124**(21):214102. DOI: http://dx.doi.org/10.1063/1.2197829

[78] Livshits E, Baer R. Physical Chemistry Chemical Physics. 2007;**9**:2932-2941. DOI: 10.1039/B617919C

[79] Peach MJG, Benfield P, Helgaker T, Tozer DJ. The Journal of Chemical Physics. 2008; **128**(4):044118–1 – 8. DOI: http://dx.doi.org/10.1063/1.2831900

[80] Zhao Y, Truhlar DG. Accounts of Chemical Research. 2008;**41**(2):157-167. DOI: 10.1021/ar700111a PMID: 18186612

[81] Stein T, Kronik L, Baer R. The Journal of Chemical Physics. 2009;**131**(24):244119. DOI: http://dx.doi.org/10.1063/1.3269029

[82] Autschbach J. Chemphyschem. 2009;**10**(11):1757-1760. DOI: 10.1002/cphc.200900268

[83] Gritsenko O, Baerends EJ. Physical Chemistry Chemical Physics. 2009;**11**:4640-4646. DOI: 10.1039/B903123E

[84] Elliott P, Goldson S, Canahui C, Maitra NT. Chemical Physics. 2011;**391**(1):110-119. DOI: http://dx.doi.org/10.1016/j.chemphys.2011.03.020

[85] Cave RJ, Zhang F, Maitra NT, Burke K. Chemical Physics Letters. 2004;**389**(1–3):39-42. DOI: http://dx.doi.org/10.1016/j.cplett.2004.03.051

[86] Mazur G, Włodarczyk R. Journal of Computational Chemistry. 2009;**30**(5):811-817. DOI: 10.1002/jcc.21102

[87] Romaniello P, Sangalli D, Berger JA, Sottile F, Molinari LG, et al. The Journal of Chemical Physics. 2009;**130**(4):044108. DOI: http://dx.doi.org/10.1063/1.3065669

[88] Dreuw A, Fleming GR, Head-Gordon M. The Journal of Physical Chemistry. B. 2003; **107**(27):6500-6503. DOI: 10.1021/jp034562r

[89] Dreuw A, Fleming GR, Head-Gordon M. Phys. Chemis. Chemical Physics. 2003;**5**:3247-3256. DOI: 10.1039/B304944B

[90] Dreuw A, Head-Gordon M. Journal of the American Chemical Society. 2004;**126**(12): 4007-4016. DOI: 10.1021/ja039556n

[91] Tozer DJ. The Journal of Chemical Physics. 2003;**119**(24):12697-12699. DOI: http://dx.doi.org/10.1063/1.1633756

[92] Stein T, Kronik L, Baer R. Journal of the American Chemical Society. 2009;**131**(8):2818-2820. DOI: 10.1021/ja8087482

[93] Ziegler T, Seth M, Krykunov M, Autschbach J. The Journal of Chemical Physics. 2008;**129**(18):184114. DOI: http://dx.doi.org/10.1063/1.3009622

[94] Iikura H, Tsuneda T, Tanai T, Hirao K. The Journal of Chemical Physics. 2001;**115**(8): 3540–3544. DOI: http://dx.doi.org/10.1063/1.1383587

[95] Song JW, Watson MA, Hirao K. The Journal of Chemical Physics. 2009;**131**(14):144108. DOI: http://dx.doi.org/10.1063/1.3243819

[96] Heyd J, Scuseria GE, Ernzerhof M. The Journal of Chemical Physics. 2003;**118**(18):8207-8216. DOI: http://dx.doi.org/10.1063/1.1564060

[97] Baer R, Neuhauser D: Physical Review Letters. 2005;**94**:043002–1–4. DOI: 10.1103/PhysRevLett.94.043002

[98] Zhao Y, Truhlar DG. The Journal of Physical Chemistry. A. 2006;**110**(49):13126-13130. DOI: 10.1021/jp066479k

[99] Seidu I, Krykunov M, Ziegler T. Journal of Chemical Theory and Computation. 2015; **11**(9):4041-4053. DOI: 10.1021/acs.jctc.5b00298

[100] Seidu I, Krykunov M, Ziegler T. The Journal of Physical Chemistry. A. 2015;**119**(21): 5107-5116. DOI: 10.1021/jp5082802

[101] Senn F, Krykunov M. The Journal of Physical Chemistry. A. 2015;**119**(42):10575-10581. DOI: 10.1021/acs.jpca.5b07075

[102] Senn F, Park YC. The Journal of Chemical Physics. 2016;**145**(24):244108–1 – 10. DOI: 10.1063/1.4972231

[103] Seidu I. Excited-State Studies with the Constricted Variational Density Functional Theory (CV-DFT) Method. PhD dissertation. University of Calgary; 2016

[104] Park YC, Senn F, Krykunov M, Ziegler T. Journal of Chemical Theory and Computation. 2016;**12**(11):5438-5452. DOI: 10.1021/acs.jctc.6b00333

[105] Ziegler T, Krykunov M, Seidu I, Park YC. In: Ferré N, Filatov M, Huix-Rotllant M, editors. Density-Functional Methods for Excited States, Vol. 368 of Top. Curr. Chem. Springer International Publishing; 2016. pp. 61-95. DOI: 10.1007/128_2014_611

[106] Ziegler T, Krykunov M, Autschbach J. Journal of Chemical Theory and Computation. 2014;**10**(9):3980-3986. DOI: 10.1021/ct500385a

[107] Hirata S, Head-Gordon M. Chemical Physics Letters. 1999;**314**(3–4):291-299. DOI: http://dx.doi.org/10.1016/S0009-2614(99)01149-5

[108] Martin RL. The Journal of Chemical Physics. 2003;**118**(11):4775-4777. DOI: http://dx.doi.org/10.1063/1.1558471

[109] Ziegler T, Krykunov M. The Journal of Chemical Physics. 2010;**133**(7):074104. DOI: http://dx.doi.org/10.1063/1.3471449

[110] Seidu I, Zhekova HR, Seth M, Ziegler T. The Journal of Physical Chemistry. A. 2012; **116**(9):2268-2277. DOI: 10.1021/jp209507n

[111] Ziegler T, Krykunov M, Cullen J. Journal of Chemical Theory and Computation. 2011; **7**(8):2485-2491. DOI: 10.1021/ct200261a

[112] Baerends E, Ziegler T, Autschbach J, Bashford D, Bérces A, et al. ADF. Theoretical chemistry, Vrije Universiteit, Amsterdam. In: The Netherlands. 2012

[113] Baerends E, T Z, Atkins A, Autschbach J, Bashford D, et al.: ADF Developers Version. Theoretical Chemistry, Vrije Universiteit, Amsterdam, The Netherlands, 2016

[114] Dreuw A, Weisman JL, Head-Gordon M. The Journal of Chemical Physics. 2003;**119**(6): 2943-2946. DOI: http://dx.doi.org/10.1063/1.1590951

[115] Ziegler T, Seth M, Krykunov M, Autschbach J, Wang F. THEOCHEM Journal of Molecular Structure. 2009;**914**(1–3):106-109. DOI: http://dx.doi.org/10.1016/j.theochem.2009.04.021

[116] Trickl T, Cronwell EF, Lee YT, Kung AH. The Journal of Chemical Physics. 1989; **91**(10):6006-6012. DOI: http://dx.doi.org/10.1063/1.457417

[117] Ben-Shlomo SB, Kaldor U. The Journal of Chemical Physics. 1990;**92**(6):3680-3683. DOI: http://dx.doi.org/10.1063/1.457824

[118] Verma P, Bartlett RJ. The Journal of Chemical Physics 2014;**140**(18):18A534. DOI: http://dx.doi.org/10.1063/1.4871409

[119] Gruening M, Gritsenko OV, van Gisbergen SJA, Baerends EJ. Chemical Physics. 2002; **116**(22):9591-9601. DOI: http://dx.doi.org/10.1063/1.1476007

[120] Autschbach J, Srebro M. Accounts of Chemical Research. 2014;**47**(8):2592-2602. DOI: 10.1021/ar500171t

[121] Krykunov M, Seth M, Ziegler T. The Journal of Chemical Physics. 2014;**140**(18):18A502. DOI: http://dx.doi.org/10.1063/1.4849397

[122] Zhekova H, Krykunov M, Autschbach J, Ziegler T. Journal of Chemical Theory and Computation. 2014;**10**(8):3299-3307. DOI: 10.1021/ct500292c

[123] Hieringer W, Görling A. Chemical Physics Letters. 2006;**419**(4–6):557-562. DOI: http://dx.doi.org/10.1016/j.cplett.2005.11.112

[124] Kobayashi R, Amos RD. Chemical Physics Letters. 2006;**420**(1–3):106-109. DOI: http://dx.doi.org/10.1016/j.cplett.2005.12.040

[125] Yanai T, Tew DP, Handy NC. Chemical Physics Letters. 2004;**393**(1–3):51-57. DOI: http://dx.doi.org/10.1016/j.cplett.2004.06.011

[126] Rudberg E, Sałek P, Helgaker T, Ågren H. The Journal of Chemical Physics. 2005; **123**(18):184108-184101-7. DOI: http://dx.doi.org/10.1063/1.2104367

[127] Tsai CW, YC S, Li GD, Chai JD. Physical Chemistry Chemical Physics. 2013;**15**:8352-8361. DOI: 10.1039/C3CP50441G

[128] Gritsenko O, Baerends EJ. The Journal of Chemical Physics. 2004;**121**(2):655-660. DOI: http://dx.doi.org/10.1063/1.1759320

[129] Maitra NT, Tempel DG. The Journal of Chemical Physics. 2006;**125**(18):184111. DOI: http://dx.doi.org/10.1063/1.2387951

[130] Kaduk B, Kowalczyk T, Voorhis TV. Chemical Reviews. 2012;**112**(1):321-370. DOI: 10.1021/cr200148b

[131] Baruah T, Olguin M, Zope RR. The Journal of Chemical Physics. 2012;**137**(8):084316. DOI: http://dx.doi.org/10.1063/1.4739269

[132] Filatov M, Huix-Rotllant M. The Journal of Chemical Physics. 2014;**141**(2):024112. DOI: http://dx.doi.org/10.1063/1.4887087

[133] Filatov M. Ensemble DFT Approach to Excited States of Strongly Correlated Molecular Systems. Cham: Springer International Publishing; 2016. pp. 97-124. DOI: 10.1007/128_2015_630

[134] Solovyeva A, Pavanello M, Neugebauer J. The Journal of Chemical Physics. 2014;**140** (16):164103. DOI: http://dx.doi.org/10.1063/1.4871301

[135] Richard RM, Herbert JM. Journal of Chemical Theory and Computation. 2011;**7**(5):1296-1306. DOI: 10.1021/ct100607w

[136] Grimme S, Parac M. Chemphyschem. 2003;**4**(3):292-295. DOI: 10.1002/cphc.200390047

[137] Angliker H, Rommel E, Wirz J. Chemical Physics Letters. 1982;**87**(2):208-212. DOI: http://dx.doi.org/10.1016/0009-2614(82)83589-6

[138] Houk KN, Lee PS, Nendel M. The Journal of Organic Chemistry. 2001;**66**(16):5517-5521. DOI: 10.1021/jo010391f

[139] Bendikov M, Duong HM, Starkey K, Houk KN, Carter EA, et al. Journal of the American Chemical Society. 2004;**126**(24):7416-7417. DOI: 10.1021/ja048919w

[140] Hajgató B, Szieberth D, Geerlings P, De Proft F, Deleuze MS. The Journal of Chemical Physics. 2009;**131**(22):224321. DOI: http://dx.doi.org/10.1063/1.3270190

[141] Hajgató B, Huzak M, Deleuze MS. The Journal of Physical Chemistry. A. 2011;**115**(33): 9282-9293. DOI: 10.1021/jp2043043

[142] Rayne S, Forest K. Computational & Theoretical Chemistry. 2011;**976**(1–3):105-112. DOI: http://dx.doi.org/10.1016/j.comptc.2011.08.010

[143] Ibeji CU, Ghosh D. Physical Chemistry Chemical Physics. 2015;**17**:9849-9856. DOI: 10.1039/C5CP00214A

[144] Anthony JE. Chemical Reviews. 2006;**106**(12):5028-5048. DOI: 10.1021/cr050966z

[145] Anthony J. Angewandte Chemie, International Edition. 2008;**47**(3):452-483. DOI: 10.1002/anie.200604045

[146] Plasser F, Pašalić H, Gerzabek MH, Libisch F, Reiter R, et al. Angewandte Chemie, International Edition. 2013;**52**(9):2581-2584. DOI: 10.1002/anie.201207671

[147] Krykunov M, Grimme S, Ziegler T. Journal of Chemical Theory and Computation. 2012;**8**(11):4434-4440. DOI: 10.1021/ct300372x

[148] Heinze HH, Görling A, Rösch N. The Journal of Chemical Physics. 2000;**113**(6):2088-2099. DOI: http://dx.doi.org/10.1063/1.482020

[149] Raghu C, Anusooya Pati Y, Ramasesha S. Physical Review B. 2002;**66**:035116–1 – 11. DOI: 10.1103/PhysRevB.66.035116

[150] Hachmann J, Dorando JJ, Avilés M, Chan GKL. The Journal of Chemical Physics. 2007;**127**(13):134309. DOI: http://dx.doi.org/10.1063/1.2768362

[151] Escudero D, Thiel W. The Journal of Chemical Physics. 2014;**140**(19):194105. DOI: http://dx.doi.org/10.1063/1.4875810

[152] Beach NA, Gray HB. Journal of the American Chemical Society. 1968;**90**(21):5713-5721. DOI: 10.1021/ja01023a011

[153] Ayers JB, Waggoner WH. Journal of Inorganic and Nuclear Chemistry. 1971;**33**(3):721-733. DOI: http://dx.doi.org/10.1016/0022-1902(71)80470-0

[154] Vancoillie S, Zhao H, Tran VT, Hendrickx MFA, Pierloot K. Journal of Chemical Theory and Computation. 2011;**7**(12):3961-3977. DOI: 10.1021/ct200597h

[155] Pierloot K, Tsokos E, Vanquickenborne LG. The Journal of Physical Chemistry. 1996; **100**(41):16545-16550. DOI: 10.1021/jp9614355

[156] Pierloot K, Praet EV, Vanquickenborne LG, Roos BO. The Journal of Physical Chemistry. 1993;**97**(47):12220-12228. DOI: 10.1021/j100149a021

[157] Formiga ALB, Vancoillie S, Pierloot K. Inorganic Chemistry. 2013;**52**(18):10653-10663. DOI: 10.1021/ic401704r. PMID: 23992205

[158] Coe BJ, Avramopoulos A, Papadopoulos MG, Pierloot K, Vancoillie S, et al. Chemistry - A European Journal. 2013;**19**(47):15955-15963. DOI: 10.1002/chem.201301380

[159] Escudero D, González L. Journal of Chemical Theory and Computation. 2012;**8**(1):203-213. DOI: 10.1021/ct200640q

[160] de Graaf C, Sousa C: Chemistry - A European Journal, 2010;**16**(15):4550-4556. DOI: 10.1002/chem.200903423

[161] Klamt A, Schüürmann G. Journal of the Chemical Society, Perkin Transactions. 1993; **2**:799-805. DOI: 10.1039/P29930000799

[162] Pye CC, Ziegler T. Theoretical Chemistry Accounts. 1999;**101**(6):396-408. DOI: 10.1007/s002140050457

[163] Su J, WH X, CF X, Schwarz WHE, Li J. Inorganic Chemistry. 2013;**52**(17):9867-9874. DOI: 10.1021/ic4009625 PMID: 23957772

[164] Dierksen M, Grimme S. The Journal of Physical Chemistry. A. 2004;**108**(46):10225-10237. DOI: 10.1021/jp047289h